

**REMARKS**

Entry of the foregoing and reconsideration of the application identified in caption, as amended, pursuant to and consistent with 37 C.F.R. §1.111 and in light of the remarks which follow, are respectfully requested.

By the above amendments, claim 1 has been amended for clarification purposes to recite that the weight percent of the water-miscible solvent is with respect to the overall solid content. This is apparent in view of the disclosure at page 3, lines 28-34 of the specification. In addition, claim 1 has been amended for clarification purposes to recite that the neutralizer is capable of reacting with a carboxylic acid group. Support for such amendment can be found in the specification at least at page 6, lines 9-21. Claim 12 has been amended for readability and grammatical purposes.

In the Official Action, claims 1-3, 7-12 and 16-20 stand rejected under 35 U.S.C. §112, second paragraph, for the reasons set forth at page 2 of the Official Action. This rejection is moot in light of the above amendments of claim 1, in which such claim has been amended to recite that the weight percent of the water-miscible solvent is with respect to the overall solid content. Accordingly, withdrawal of the above rejection is respectfully requested.

Claims 1-3, 7-12 and 16-22 stand rejected under 35 U.S.C. §112, first paragraph, for the reasons set forth at pages 2-3 (section 3) of the Official Action. In this regard, it is noted that the Examiner's comments appear to be only directed to claim 19 which recites the tensile modulus of the polyurethane. With regard to the recited tensile modulus characteristic, Applicants note that due to the existence of physical crosslinking and/or molecular entanglement in such exemplary polyurethane, the tensile modulus of such polyurethane is capable of being measured at a temperature above the melting point thereof. In addition, Applicants note that the tensile modulus of various polyurethanes can be measured at temperatures exceeding the melting points thereof. See, e.g., *Y. Zhu et al*, Chinese Journal of Polymer Science, Vol. 24, No. 2 (2006), pp.

173-186 (copy attached), and in particular Figure 5 at page 178. Accordingly, for at least the above reasons, withdrawal of the above rejection is respectfully requested.

Claims 1-3, 7-12 and 16-22 stand rejected under 35 U.S.C. §112, first paragraph, for the reasons set forth at pages 3-4 (section 4) of the Official Action. Withdrawal of the above rejection is respectfully requested for at least the following reasons.

Applicants respectfully submit that a polyurethane having a glass transition point as low as, for example, -30°C can be obtained with the use of the raw materials disclosed in the instant specification. Moreover, contrary to the Examiner's assertion, conventional shape-memory polymers formed from polyurethanes having a glass transition temperature as low as -30°C have been obtained. See, e.g., *A. Lendlein et al*, *Angewandte Chemie International Edition*, Vol. 41 (2002), pp. 2034-2057 (copy attached), and in particular Table 2 at page 2044. Accordingly, in view of the above, withdrawal of this rejection is respectfully requested.

Claims 1-3, 7-12 and 16-22 stand rejected under 35 U.S.C. §112, first paragraph, for the reasons set forth at pages 4-5 (section 5) of the Official Action. While Applicants disagree with the Examiner's assertions for the reasons already made of record, in an effort to expedite prosecution, claim 1 has been amended to recite that the neutralizer is capable of reacting with a carboxylic acid group, in accordance with the Examiner's suggestion.

The Examiner has asserted that Applicants' disclosure does not sufficiently enable one skilled in the art how to produce a polyurethane having the properties set forth in claims 19-22. In this regard, it is noted that the standard for complying with the provisions of the first paragraph of 35 U.S.C. §112 is well established. For example, it is not necessary to "enable one of ordinary skill in the art to make and use a perfected, commercially viable embodiment. . . ." *CFMT, Inc. v. Yieldup Int'l Corp.*, 349 F.3d 1333, 1338 (Fed. Cir. 2003). "Detailed procedures for making and using the invention may not be necessary if the description of the invention itself is sufficient to permit those skilled in the art to make and use the invention." M.P.E.P. §2164.

Moreover, "the scope of enablement must only bear a 'reasonable correlation' to the scope of the claims." M.P.E.P. §2164.08.

Applicants respectfully submit that, upon review of the applicable standard of enablement under 35 U.S.C. §112, it is apparent that the level of detail and description suggested in the Official Action, e.g., the specific ratios of reactants and the selection of specific reactants, is simply not required in the present case. Accordingly, for at least the above reasons, withdrawal of the rejection is respectfully requested.

Claims 1-3, 7-12 and 16-22 stand rejected under 35 U.S.C. §102(b) as being anticipated by U.S. Patent No. 6,239,213 (*Ramanathan et al*). Claims 21 and 22 stand rejected under 35 U.S.C. §102(b) as being obvious over U.S. Patent No. 5,270,433 (*Klauck et al*). Withdrawal of the above rejections is respectfully requested for at least the following reasons.

It is well established that "[a] claim is anticipated only if each and every element as set forth in the claim is found, either expressly or inherently described, in a single prior art reference." *Verdegaal Bros. v. Union Oil Co. of California*, 2 USPQ2d 1051, 1053 (Fed. Cir. 1987). For an anticipation to exist, "[t]he identical invention must be shown in as complete detail as is contained in the . . . claim." *Richardson v. Suzuki Motor Co.*, 9 USPQ2d 1913, 1920 (Fed. Cir. 1989).

In the present case, the Patent Office has relied on *Ramanathan et al*'s disclosure of reacting branched polyester polyol, an ionic group bearing organic compound and an organic diisocyanate, and has asserted that such components may be reacted sequentially to form block copolymers (Official Action at page 6). However, independent claim 1 recites heating a first mixture formed from mixing a difunctional alcohol with a difunctional isocyanate, and thereafter adding a chain extender to the heated first mixture. *Ramanathan et al* simply has no disclosure of the addition of a chain extender after heating of the first mixture as presently claimed. In this regard, it is noted that the claimed process recites the use of both a difunctional alcohol in step a)

and a chain extender in step c), i.e., the recited chain extender is distinct from the recited difunctional alcohol. Moreover, it is believed that the above differences in the claimed and disclosed processes lead to different products.

*Klauck et al* requires the use of  $\alpha,\alpha,\alpha',\alpha'$ -tetramethyl xylene diisocyanate. This component, which has been characterized by the Patent Office as an aliphatic diisocyanate, is now excluded from the present claims. Furthermore, the Patent Office has not established with the requisite certainty, that the polyurethane of *Klauck et al* inherently possesses the claimed tensile modulus characteristic.

In this regard, the Patent Office's burden of proof for properly alleging an inherent disclosure is well established. "To establish inherency, the extrinsic evidence 'must make clear that the missing descriptive matter is necessarily present in the thing described in the reference, and that it would be so recognized by persons of ordinary skill. Inherency, however, may not be established by probabilities or possibilities. The mere fact that a certain thing may result from a given set of circumstances is not sufficient.'" *In re Robertson*, 49 USPQ2d 1949, 1950-51 (Fed. Cir. 1999) (emphasis added). "In relying upon the theory of inherency, the examiner must provide a basis in fact and/or technical reasoning to reasonably support the determination that the allegedly inherent feature necessarily flows from the teachings of the applied prior art." *Ex Parte Levy*, 17 USPQ2d 1461, 1464 (Bd. Pat. App. & Inter. 1990) (emphasis in original). In the present case, and as discussed above, the difunctional isocyanate used to form the claimed polyurethane differs from the material employed in *Klauck et al* (Official Action at page 4). The Patent Office has not provided a sufficient explanation or scientific reasoning as to why it is certain, given such different reactants, that the resulting polyurethane of *Klauck et al* is identical to the claimed polyurethane. It is apparent that the Patent Office has failed to meet its burden of proof for establishing inherency of this claimed feature.

For at least the above reasons, *Ramanathan et al* and *Klauck et al* fail to constitute an anticipation of the claims. Accordingly, withdrawal of the above rejections is respectfully requested.

From the foregoing, further and favorable action in the form of a Notice of Allowance is believed to be next in order, and such action is earnestly solicited. If there are any questions concerning this paper or the application in general, the Examiner is invited to telephone the undersigned.

Respectfully submitted,

BUCHANAN INGERSOLL & ROONEY PC

Date: May 9, 2007

By: 

Roger H. Lee  
Registration No. 46317

P.O. Box 1404  
Alexandria, Virginia 22313-1404  
(703) 836-6620

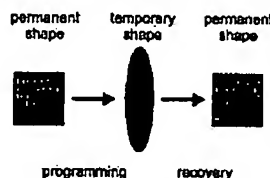
Reprint

# ANGEWANDTE CHEMIE

A Journal of the  
Gesellschaft  
Deutscher Chemiker

## INTERNATIONAL EDITION

### Shape-Memory Polymers



Upon exposure to an external stimulus, shape-memory polymers can change their shape (see scheme). This ability opens up numerous fields of application, such as intelligent, bulky implants, which can be inserted in a compressed, temporary shape into the body through a small incision, or auto bodies, which could be brought back to their original shape after a collision by a simple heat treatment. The current state and the potential of this technology is summarized in the article.

A. Lendlein,\* S. Kelch ..... 2034-2057

**Keywords:** block copolymers •  
elastomers • materials science •  
polymers • shape-memory polymers

**2002-41/12**

WILEY-VCH Verlag GmbH, Weinheim

 **WILEY-VCH**

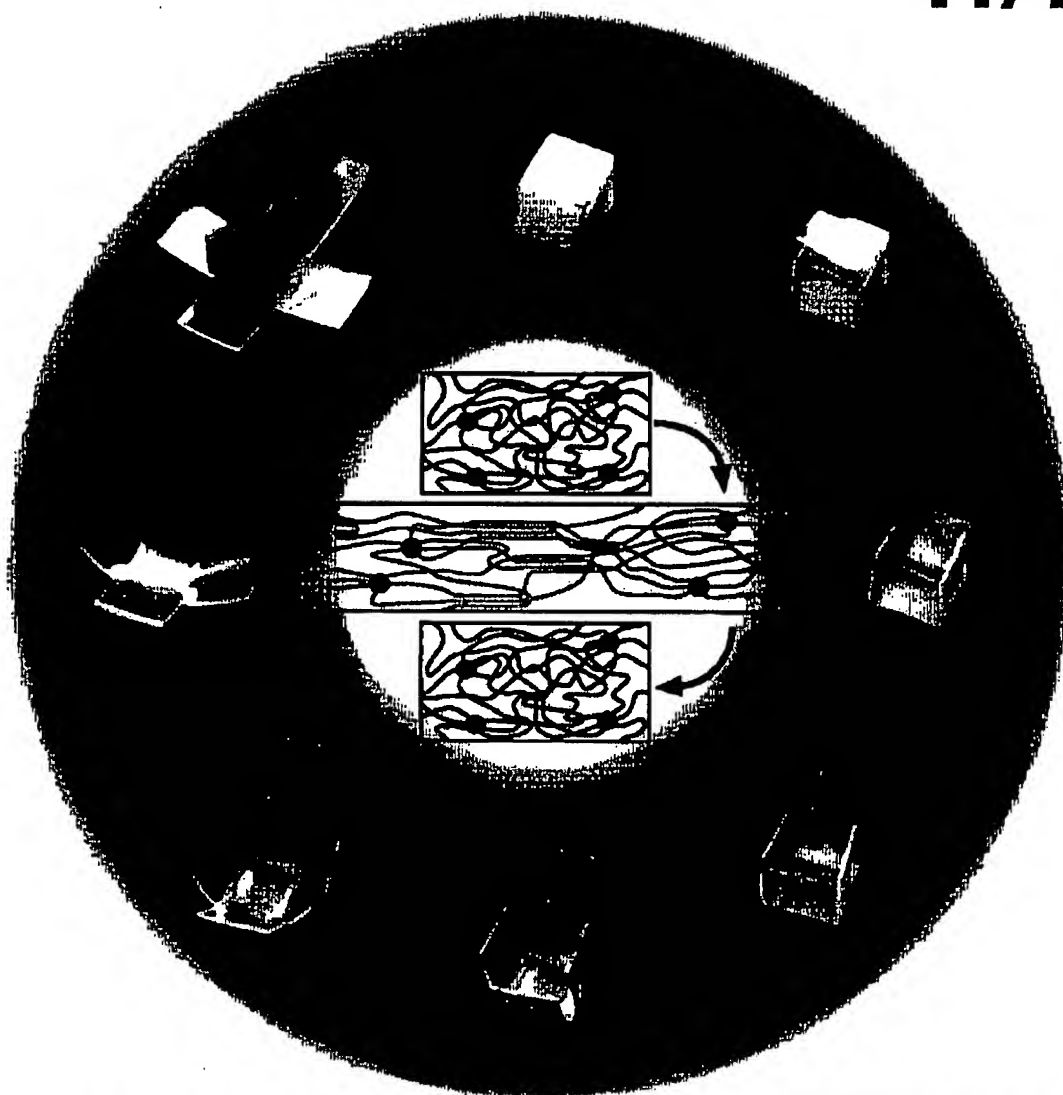
D 3461

# ANGEWANDTE CHEMIE

A Journal of the  
Gesellschaft  
Deutscher Chemiker

INTERNATIONAL EDITION

**2002**  
**41/12**



Angewandte on the Web:  
[www.angewandte.com](http://www.angewandte.com) (Homepage) and  
[www.interscience.wiley.com/jpages/0044-8249](http://www.interscience.wiley.com/jpages/0044-8249)

 **WILEY-VCH**

**Nobel Lectures**

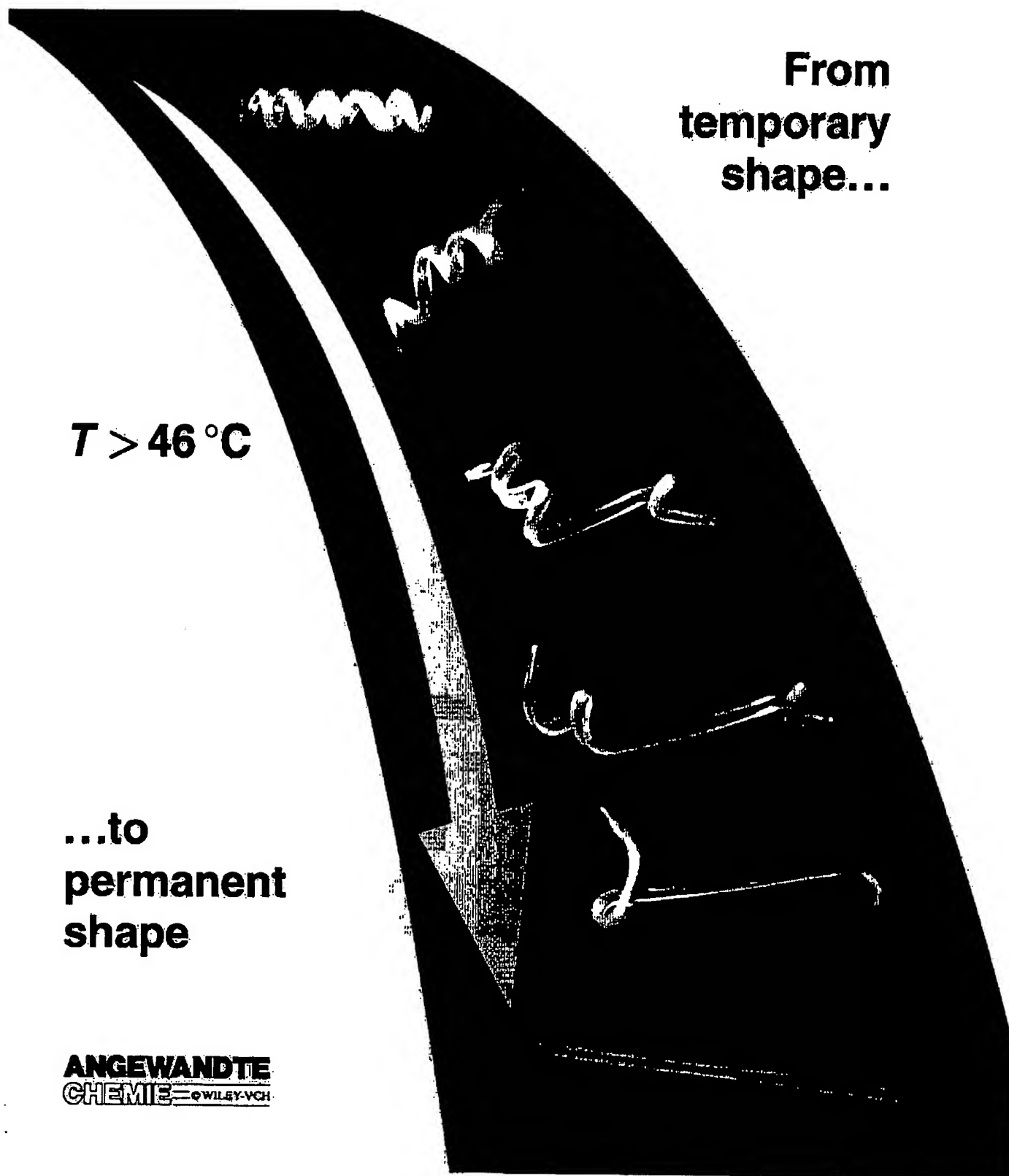
# Shape-Memory Effect

From  
temporary  
shape...

$T > 46^{\circ}\text{C}$

...to  
permanent  
shape

**ANGEWANDTE  
CHEMIE** — WILEY-VCH



## Shape-Memory Polymers

Andreas Lendlein\* and Steffen Kelch

Material scientists predict a prominent role in the future for self-repairing and intelligent materials. Throughout the last few years, this concept has found growing interest as a result of the rise of a new class of polymers. These so-called shape-memory polymers by far surpass well-known metallic shape-memory alloys in their shape-memory properties. As a consequence of the relatively easy manufacture and programming of shape-memory polymers,

these materials represent a cheap and efficient alternative to well-established shape-memory alloys. In shape-memory polymers, the consequences of an intended or accidental deformation caused by an external force can be ironed out by heating the material above a defined transition temperature. This effect can be achieved because of the given flexibility of the polymer chains. When the importance of polymeric materials in our daily life

is taken into consideration, we find a very broad, additional spectrum of possible applications for intelligent polymers that covers an area from minimally invasive surgery, through high-performance textiles, up to self-repairing plastic components in every kind of transportation vehicles.

**Keywords:** block copolymers • material science • polymers • shape-memory polymers

### 1. Introduction

Shape-memory materials are stimuli-responsive materials. They have the capability of changing their shape upon application of an external stimulus. A change in shape caused by a change in temperature is called a thermally induced shape-memory effect. The main focus of this review article is on thermoresponsive shape-memory polymers. The shape-memory effect is not related to a specific material property of single polymers; it rather results from a combination of the polymer structure and the polymer morphology together with the applied processing and programming technology. Shape-memory behavior can be observed for several polymers that may differ significantly in their chemical composition. However, only a few shape-memory polymers are described in the literature. The process of programming and recovery of a shape is shown schematically in Figure 1. First, the polymer is conventionally processed to receive its permanent shape. Afterwards, the polymer is deformed and the intended temporary shape is fixed. This process is called programming. The programming process either consists of heating up the sample, deforming, and cooling the sample, or drawing the

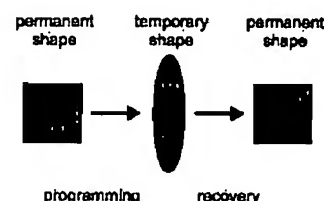


Figure 1. Schematic representation of the thermally induced one-way shape-memory effect. The permanent shape is transferred to the temporary shape by the programming process. Heating the sample to a temperature above the switching transition  $T_{\text{trans}}$  results in the recovery of the permanent shape.

sample at a low temperature (so called "cold drawing"). The permanent shape is now stored while the sample shows the temporary shape. Heating up the shape-memory polymer above a transition temperature  $T_{\text{trans}}$  induces the shape-memory effect. As a consequence, the recovery of the stored, permanent shape can be observed. Cooling down the polymer below the transition temperature leads to solidification of the material, however, no recovery of the temporary shape can be observed. The effect described is named as a one-way shape-memory effect. By further programming, including mechanical deformation, the work piece can be brought into a temporary shape again. This new temporary shape does not necessarily match the first temporary shape.

In Figure 2 a picture sequence demonstrates impressively the performance of shape-memory polymers. The permanent shape of the polymers formed from 1 and 2 is that of a rod,

[\*] Dr. A. Lendlein, Dr. S. Kelch  
Institut für Chemie  
GKSS Forschungszentrum  
Kantstrasse 55, 14513 Teltow (Germany)  
Fax: (+49) 3328 352 452  
E-mail: lendlein@gkss.de

which has been deformed to a spiral (temporary shape) during the programming process. Under the influence of hot air having a temperature of 70°C the permanent shape is recovered as soon as the switching temperature  $T_{\text{switch}}$  is reached. The permanent shape is recovered with a precision of more than 99% with appropriately optimized programming conditions. This precision makes these materials suitable for highly demanding applications.<sup>[1]</sup>

Since the 1960s, polyethylene that is covalently cross-linked by means of ionizing radiation has found broad application as heat-shrinking film or tubing, especially for the insulation of electric wires or as protection against corrosion of pipe lines.<sup>[2–7]</sup> These materials are marketed under the catchphrase "heat-shrinkable materials". The mechanism of the heat-shrinking process is in analogy with the thermally induced shape-memory effect. Here, the permanent shape is also fixed by covalent cross-links and the switching process is controlled by the melting temperature of the polyethylene crystallites.

More and more reports about linear, phase-segregated multiblock copolymers, mostly polyurethanes, can be found in

the literature under the name of the generic term "shape-memory polymers" (see Section 2.4.1). These elastic materials show at least two separated phases. The phase showing the highest thermal transition  $T_{\text{perm}}$  acts as the physical cross-link and is responsible for the permanent shape. Above this temperature the polymer melts and can be processed by conventional processing techniques such as extrusion or injection molding. A second phase serves as a molecular switch and enables the fixation of the temporary shape. The transition temperature for the fixation of the switching segments can either be a glass transition ( $T_g$ ) or a melting temperature ( $T_m$ ). After forming the material above the switching temperature, but below  $T_{\text{perm}}$ , the temporary shape can be fixed by cooling the polymer below the switching temperature. Heating up the material above  $T_{\text{switch}}$  again cleaves the physical cross-links in the switching phase. As a result of its entropy elasticity (see Section 2.1.3) the material is forced back to its permanent shape. Polyurethanes with shape-memory properties have found application as, for example, components in auto chokes. In this application it is

*Andreas Lendlein, born in 1969 in Bendorf (Germany), studied chemistry at the Johannes Gutenberg University of Mainz (1988–1993). In 1993–1996 he did his dissertation with Prof. Dr. Ulrich W. Suter at the material science department of the Swiss Federal Institute of Technology (ETH) in Zurich, Switzerland. In his Ph.D. thesis he dealt with degradable and biocompatible multiblock copolymers with hard segments based on bacterially produced polyesters. In 1996, after a short post-doctoral stay in Zurich, he was awarded the ETH Medal, and in 1997 he moved, as a visiting scientist, to the group of Prof. Dr. Robert Langer at the Massachusetts Institute of Technology (MIT) in Cambridge, USA. Since*



A. Lendlein

S. Kelch

*1998 he has been head of the department for the Development and Engineering of New Biomaterials, which he established at the German Wool Research Institute at the RWTH Aachen and he habilitated from the Chair of Textile Chemistry and Macromolecular Chemistry at the University of Technology, Aachen. He recently accepted a position as full professor at the University of Potsdam (Germany) and as director of the Institute of Chemistry at the GKSS Research Center in Teltow (Germany). Currently, he is working on the development of intelligent polymers, especially block copolymers and multiphase covalent networks, the processing of these materials, as well as their application in the biomedical field. Besides his academic career, in 1998 he founded, together with Robert Langer, the start-up company mnemoScience GmbH of Aachen, which he runs as managing director. He has received numerous grants, among others, Studienstiftung des deutschen Volkes (1989–1993), Früz-Ter-Meer Stiftung (1989–1992), Gottlieb Daimler- und Karl Benz-Stiftung (1993–1996), as well as the Liebig Stipendium of the Fonds der Chemischen Industrie (1997–1999). In 1998 he was laureate in the BioFuture Contest of the Ministry for Education and Research (BMBF), in 1999 he was honored by Pinguin Stiftung, in 2000 he received the Hermann-Schnell award of the GDCH, as well as the Innovationspreis of Zenit e. V.*

*Steffen Kelch, born in 1967 in Mannheim (Germany), studied chemistry from 1989 to 1995 at the University of Karlsruhe (TH) and did his dissertation from 1995–1999 at the Polymer Institute there in the group of Prof. Dr. Matthias Rehahn. In his Ph.D. thesis he dealt with the synthesis and characterization of high molecular weight coordination polymers. In 1996 he worked in the group of PD Dr. Walter Caseri at the Institute of Polymers of the Swiss Federal Institute of Technology in Zurich on the modification of inorganic surfaces. During his doctorate and thereafter as a research associate at the German Plastics Institute (DKI) in Darmstadt he worked on the characterization of polyurethane networks. Since 2000 he has worked as a research scientist in the department for the Development and Engineering of New Biomaterials at the German Wool Research Institute at the University of Technology Aachen.*

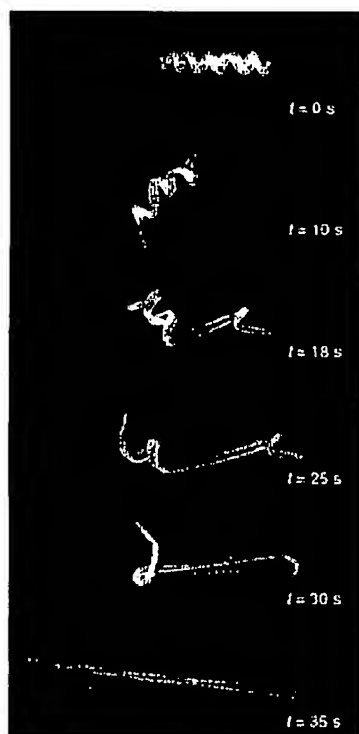
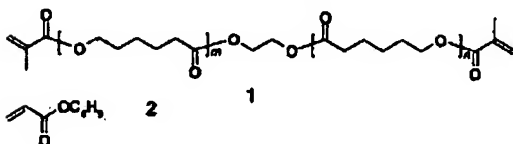


Figure 2. Transition from the temporary shape (spiral) to the permanent shape (rod) for a shape-memory network that has been synthesized from poly( $\epsilon$ -caprolactone) dimethacrylate (1) and butylacrylate (2; co-monomer content: 50 wt %; see Section 2.6.2). The switching temperature of this polymer is 46 °C. The recovery process takes 35 s after heating to 70 °C.



not the shape-memory effect that is used, but the property of the polymer to soften upon being heated up above the switching temperature.<sup>[8–19]</sup>

A substantially new development in connection with the design of shape-memory polymers are polymer systems. These are families of polymers in which macroscopic properties (for example, mechanical properties or  $T_{\text{trans}}$ ) can be controlled by a specific variation of molecular parameters. This makes it possible to tailor the specific combination of the properties of the shape-memory polymers that are required for specific applications just by a slight variation of the chemical composition. The shape-memory material presented in Figure 2 belongs to a family of multiphase polymer networks that are biocompatible and biodegradable. Such materials are highly interesting for applications in the field of minimally invasive surgery (see Section 2.6).

There are other classes of materials such as metallic alloys, ceramics, and gels that show thermoresponsive shape-memory properties. A short overview about these other shape-memory materials is given before shape-memory polymers are discussed in detail.

## 1.1. Metal Alloys

The one-way shape-memory effect as described at the beginning was observed for the first time by Chang and Read in 1951 for a gold–cadmium alloy.<sup>[20]</sup> In 1963 Buehler et al. described the shape-memory effect of nitinol, an equiatomic nickel–titanium alloy.<sup>[21]</sup> Here, the shape-memory effect is based on a martensitic phase transition taking place without diffusion (Figure 3). To generate the martensitic phase the

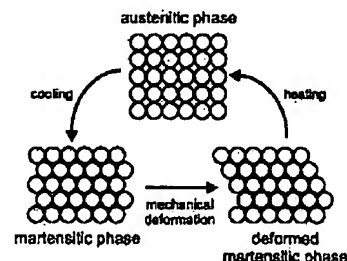


Figure 3. Schematic representation of the mechanism of the shape-memory effect for metallic alloys based on a martensitic phase transformation.

material is cooled from a high temperature or parent phase showing a cubic symmetry (austenitic phase) down to a low temperature phase with lower symmetry (martensitic phase). The formation of the martensitic phase can be controlled by a temperature program which includes heating to temperatures up to 450 °C. The temporary shape of the material can now be produced by deformation of the material in the martensitic phase. The austenitic phase is reached upon heating the sample above the phase transition temperature and a recovery of the original external shape for deformations of up to 8 % can be observed.

Since nitinol is an equiatomic Ni–Ti alloy, possible fluctuations in stoichiometry have a strong influence on the resulting properties of the material. A deviation in the nickel content of 1 atom % can shift the switching temperature up to 100 K. Besides the one-way shape-memory effect, nitinol exhibits so called superelasticity. Superelasticity is based on the phenomenon that the martensitic phase is not stable above a certain temperature in the absence of an external force. Above this temperature an external deformation will spontaneously be recovered.<sup>[22a,b,d, 23–29]</sup>

The Ni–Ti and Cu–Zn–Al alloys all found technical application. Nitinol is widely used for the manufacture of surgical devices and implants because of its biocompatibility.<sup>[22b, 30, 31]</sup> Cu–Zn–Al alloys are often used for nonmedical applications as a result of their advantageous thermal and electrical conductivity and their better ductility. Cu–Al–Ni as well as iron-based alloys such as Fe–Mn–Si, Fe–Cr–Ni–Si–Co, Fe–Ni–Mn, or Fe–Ni–C alloys have also been investigated in regard to their shape-memory properties. Fe–Mn–Si alloys, in particular, find applications as materials for screwed joints that can be heated after being screwed together to obtain further compression.<sup>[22c,d, 23]</sup>

Metallic alloys with shape-memory properties can show a two-way shape-memory effect after a certain “thermal train-

ing". In this case the material does not only "remember" the external shape in the parent phase but also the external shape in the martensitic phase. By this, it is possible to produce a defined structure at a defined temperature that has been programmed before.<sup>[22a, 27, 30]</sup>

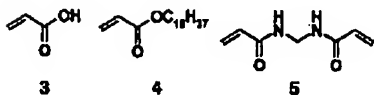
## 1.2. Ceramics

With certain  $\text{ZrO}_2$  ceramics, the transition from a tetragonal to a monoclinic structure occurs as a martensitic phase transition which is induced thermally or by the application of stress. These materials are called martensitic ceramics. The transformation back from the monoclinic to the tetragonal symmetry can occur thermoelastically, which is why martensitic ceramics show a thermoresponsive shape-memory effect.<sup>[22a, 23, 24]</sup>

## 1.3. Gels

A remarkable property of polymer gels is their ability to react to changes in the external conditions by considerable volume changes, swelling or shrinkage. The external stimulus is not only limited to temperature changes. Volume changes can also be triggered by a variation in the pH value, the ionic strength, or the quality of the solvent. In addition to this, it is possible to stimulate certain gels by the application of electric fields or light. The crucial point with gels is their poor mechanical stability.<sup>[32–45]</sup>

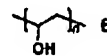
Hydrogels with hydrophobic, crystallizable side chains, and cross-linked poly(vinyl alcohols) show a thermoresponsive one-way shape-memory effect.<sup>[32, 33, 37, 39, 40]</sup> Hydrogels formed from copolymerized acrylic acid **3** and stearyl acrylate (**4**) cross-linked with methylenebisacrylamide (**5**) show a strong temperature dependence in their mechanical properties.



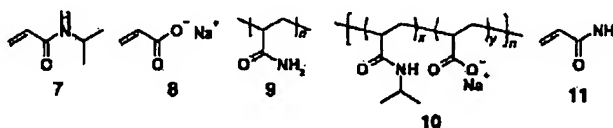
Below 25°C these polymers behave like tough polymers, while above 50°C softening enables the materials to be extended up to 50%. The softening results in a decrease of the elastic modulus by three orders of magnitude. The mechanical stability below 50°C arises from the crystalline packing of the stearyl side chains. Above this temperature, the aliphatic side chains are amorphous and contribute to the flexibility of the hydrogels. The stretched shape can be maintained by applying the deformation force during the cooling process. When the material is heated up again above the transition temperature the one-way shape-memory effect takes place and the external shape in which the material was produced initially is recovered. The permanent shape is predetermined by the covalent polymer network.<sup>[34, 39]</sup>

Linear poly(vinyl alcohol) molecules form hydrogels as a result of the formation of physical cross-links through hydro-

gen bonds and microcrystallites. Above a temperature of 50°C the physical cross-links melt and results in an increasing loss of stability. Above a temperature of 80°C the physically cross-linked hydrogels become soluble in water. Chemically cross-linked hydrogels whose permanent shape is stable above 80°C can be obtained by cross-linking the poly(vinyl alcohol) **6** with glutaraldehyde. After melting the physical cross-links in boiling water, these chemically cross-linked hydrogels can be stretched by 200%. By immersion of the system in methanol, a poor solvent, the elongation, and thus the temporary shape, can be fixed by deswelling and formation of physical cross-links. The permanent shape can be recovered by exposing the gel to boiling water.<sup>[32]</sup>



An example of materials with a thermally induced two-way shape-memory effect are modulated gels. Such gels consist of layers and can perform even more complex shape changes. They contain two types of layers: a thermosensitive control layer (control element) and a substrate layer (substrate element) which is not sensitive to changes in temperature. The control layer consists of an ionic gel made from the copolymer **10** prepared from *N*-isopropylacrylamide (NIPAA, **7**) and sodium acrylate (**8**) cross-linked with methylenebisacrylamide (**5**). A tenfold change in volume can be reached as a consequence of a thermally induced abrupt change in the gels microstructure. The gel is swollen below the lower critical



solution temperature (LCST) of 37°C. Exceeding this temperature causes shrinkage of the gel and the resulting decrease in the thermodynamic quality of the solvent produces a polymer-rich phase. The substrate layer can consist of a gel formed from polyacrylamide (PAAM) cross-linked with **5**. At temperatures above 37°C, the control layer shrinks drastically while the substrate layer does not undergo any noticeable changes in volume. To connect the two different layers, one side of the control layer, which consists of cross-linked copolymer **10**, is exposed to an aqueous solution of acrylamide (**11**). In this way, the acrylamide solution diffuses into the control layer for a certain time period. The acrylamide is then polymerized by the addition of a radical initiator and **5** to form an interpenetrating network. The bigel strip bends uniformly upon heating to form an arch. A further rolling-up of the gel structure can be realized by an additional increase in temperature or by producing a longer sample. The change in shape is reversible and the system can switch between two defined shapes depending on whether it is below or above the transition temperature. By producing a modulated gel consisting of several alternating layers it is possible to obtain spirally, cylindrically, wavy structures, or any kind of bent, ribbonlike structure.<sup>[35, 41]</sup>

## 2. Thermally Induced Shape-Memory Effect in Polymers

Before the molecular mechanism of the thermally induced shape-memory effect is explained in detail, the basic principles of entropy elasticity are discussed. Methods for the quantification of shape-memory properties are presented and the corresponding physical quantities are introduced based on a description of the macroscopic shape-memory effect. A structured overview of thermoplasts and polymer networks that show shape-memory properties will be concluded by a summary of current research work in the field of shape-memory polymers. Polymers developed for biomedical applications in particular will be focused upon.

### 2.1. Thermodynamic Aspects Significant for the Shape-Memory Effect of Polymers

#### 2.1.1. Chain Conformation of Linear, Amorphous Polymers

In the amorphous state, polymer chains take up a completely random distribution in the matrix, without the restriction that is given by the order of crystallites in semicrystalline polymers. All possible conformations of a polymer chain have the same inner energy. If  $W$  expresses the probability of a conformation, a strongly coiled conformation, which is the state of maximum entropy, represents the most probable state for an amorphous linear polymer chain according to the Boltzmann equation [Eq. (1),  $S$  = entropy;  $k$  = Boltzmann constant].<sup>[46]</sup>

$$S = k \ln W \quad (1)$$

#### 2.1.2. Transition from the Glassy State to the Rubber-Elastic State

In the glassy state all movements of the polymer segments are frozen. The transition to the rubber-elastic state occurs upon increasing the thermal activation, which means that the rotation around the segment bonds becomes increasingly unimpeded. This situation enables the chains to take up one of the possible, energetically equivalent conformations without disentangling significantly. The majority of the macromolecules will form compact random coils because this conformation is entropically favored and, as a result, much more probable than a stretched conformation (see Section 2.1.1).

In this elastic state a polymer with sufficient molecular weight ( $M_n > 20000$ ) stretches in the direction of an applied external force. If the tensile stress is only applied for a short time interval, the entanglement of the polymer chains with their direct neighbors will prevent a large movement of the chain. Consequently, the sample recovers its original length when the external stress is released. In this way, the sample shows a kind of memory for the nonstretched state. This recovery is sometimes called "memory effect", and is based on the sample's tendency to return to its original, most randomly coiled state that represents the most probable state. However, if the external tensile stress is applied for a longer

time period, a relaxation process will take place which results in a plastic, irreversible deformation of the sample because of slipping and disentangling of the polymer chains from each other. The tendency of the polymer chains to disentangle and to slip off each other into new positions enables the segments to undergo a relaxation process and to form entropically more favorable random coils.

In a similar way, an increasing rise in temperature above the glass transition temperature favors a higher segment mobility and a decrease in the mechanical stress in the elastic material being stretched by an external force.<sup>[47, 48]</sup>

#### 2.1.3. Entropy Elasticity

The described slipping or flow of the polymer chains under stress can be stopped almost completely by cross-linking the chains. The cross-linkage points act as anchors or "permanent entanglements" and prevent the chains from slipping from each other. The cross-links can either be chemical and/or physical. Those materials are called elastomers.

Chemically cross-linked polymers form insoluble materials which swell in good solvents. Their shape is fixed during the cross-linking and can not be changed afterwards.

Thermoplastic elastomers contain physical netpoints. A requisite for the formation of the netpoints is the existence of a certain morphology of a phase-separated material, as found for block copolymers containing thermodynamically immiscible components. The highest thermal transition  $T_{perm}$  is related to the hard-segment-forming phase. If this thermal transition is not exceeded, these domains will stabilize the permanent shape by acting as physical netpoints in the material. Thermoplastic elastomers are very soluble in suitable solvents and can be processed from the melt.

Besides the netpoints, networks contain flexible components in the form of amorphous chain segments. If the glass transition temperature of these segments is below the working temperature, the networks will be elastic. They show entropy elasticity and can be stretched with a loss of entropy. The distance between netpoints increase during stretching and they become oriented. As soon as the external force is released, the material returns to its original shape and gains back the entropy lost before. As a result, the polymer network is able to maintain the mechanical stress in equilibrium.

Elastomers exhibit some extraordinary properties: they warm up when they are stretched; the elastic modulus increases upon heating; the coefficient of thermal expansion for a stretched elastomer is negative above the glass transition temperature; below the  $T_g$  value the sample behaves like a glass and contracts if it is further cooled down (Figure 4). While the coefficient of thermal expansion is negative for a stretched sample, it is positive for an unloaded sample.

The inner energy of an ideal elastomer will not change if it is stretched. For this reason, the Helmholtz equation for the free energy  $U$  is reduced according to

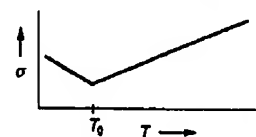


Figure 4. Plot of the stress  $\sigma$  in an elastomer which is stretched and then kept under constant strain over a temperature range above and below the  $T_g$  value.

Equation (2). From the stress-strain behavior of a polymer network with a low degree of cross-linking and netpoints that

$$U = -T\Delta S \quad (2)$$

are sufficiently far away from each other, the change in free energy for the stretching of a standard volume is given by Equation (3).  $N$  is the number of chain segments between the netpoints and  $\lambda_x$ ,  $\lambda_y$ , and  $\lambda_z$  represent the elongation ratios in three dimensions ( $\lambda = l/l_0$ ), where  $l$  represents the length of the segments between the netpoints in the stretched state, and  $l_0$  represents the length of the segments in the unloaded state.<sup>[46, 47]</sup>

$$U = \frac{1}{2} NkT(\lambda_x^2 + \lambda_y^2 + \lambda_z^2 - 3) \quad (3)$$

## 2.2. Molecular Mechanism of the Shape-Memory Effect of Polymers

An elastomer will exhibit a shape-memory functionality if the material can be stabilized in the deformed state in a temperature range that is relevant for the particular application. This can be reached by using the network chains as a kind of molecular switch. For this purpose the flexibility of the segments should be a function of the temperature. One possibility for a switch function is a thermal transition ( $T_{\text{trans}}$ ) of the network chains in the temperature range of interest for the particular application. At temperatures above  $T_{\text{trans}}$  the chain segments are flexible, whereas the flexibility of the chains below this thermal transition is at least partly limited. In the case of a transition from the rubber-elastic or viscous state to the glassy state, the flexibility of the entire segment is limited. If the thermal transition chosen for the fixation of the temporary shape is a melting point, strain-induced crystallization of the switching segment can be initiated by cooling the material which has been stretched above the  $T_{\text{trans}}$  value. The crystallization achieved is always incomplete, which means that a certain amount of the chains remains amorphous. The crystallites formed prevent the segments from immediately reforming the coil-like structure and from spontaneously recovering the permanent shape that is defined by the netpoints. The permanent shape of shape-memory networks is stabilized by covalent netpoints, whereas the permanent shape of shape-memory thermoplasts is fixed by the phase with the highest thermal transition at  $T_{\text{perm}}$ .

The molecular mechanism of programming the temporary form and recovering the permanent shape is demonstrated schematically in Figure 5 for a linear multiblock copolymer, as well as for two covalently cross-linked polymer networks.

The "memory effect" mentioned in Section 2.1.2 is not a shape-memory effect. This expression describes the property of an elastomer one would not expect for an amorphous polymer chain. The "memory effect" represents a problem in the processing of non-vulcanized natural rubber. In the case of a quick deformation of the amorphous material by a sudden subsequent decrease or removal (or reduction) of the external force, the polymer re-forms its original shape. Such polymers

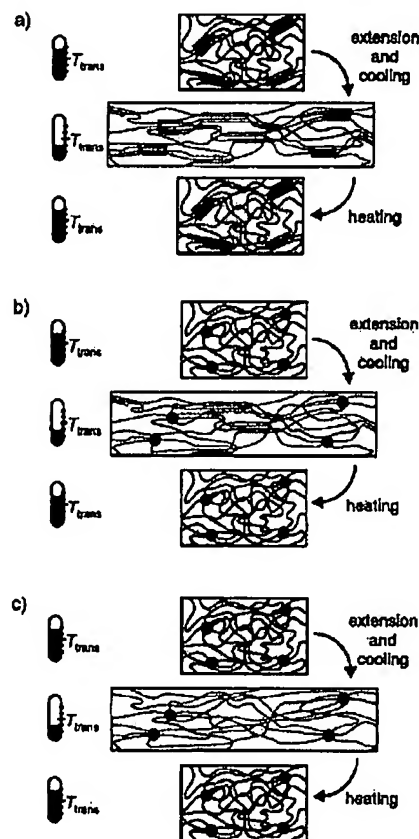


Figure 5. Schematic representation of the molecular mechanism of the thermally induced shape-memory effect for a) a multiblock copolymer with  $T_{\text{trans}} = T_m$ , b) a covalently cross-linked polymer with  $T_{\text{trans}} = T_g$ , and c) a polymer network with  $T_{\text{trans}} = T_g$ . If the increase in temperature is higher than  $T_{\text{trans}}$  of the switching segments, these segments are flexible (shown in red) and the polymer can be deformed elastically. The temporary shape is fixed by cooling down below  $T_{\text{trans}}$  (shown in blue). If the polymer is heated up again, the permanent shape is recovered.

will also exhibit a shape-memory effect if a suitable programming technique is applied. In this case, temporary entanglements of the polymer chains which act as physical netpoints can be used for the fixation of the permanent shape. This thermal transition can be used as a switching transition if the glass transition of the amorphous material is in the temperature range that is relevant for a specific application. In Section 2.4.2 this shape-memory mechanism is explained for a high molecular weight, amorphous polynorbornene.

## 2.3. Macroscopic Shape-Memory Effect and Thermomechanical Characterization

### 2.3.1. Cyclic, Thermomechanical Characterization

The shape-memory effect can be quantified by cyclic, thermomechanical investigations. The measurements are performed by means of a tensile tester equipped with a thermochamber. In this experiment, different test protocols

are applied that differ, for example, in the programming procedure (cold drawing at  $T < T_{\text{trans}}$  or temporarily heating up of the test piece to  $T > T_{\text{trans}}$ ) or in the control options (stress or strain controlled). A single cycle includes programming the test piece and recovering its permanent shape. A typical test protocol is as follows: first, the test piece is heated up to a temperature  $T_{\text{high}}$  above the switching temperature  $T_{\text{trans}}$  and is stretched to the maximum strain  $\epsilon_m$ . In the case of thermoplasts it is important not to exceed the highest thermal transition  $T_{\text{perm}}$  which would cause the polymer sample to melt. The sample is cooled down below the transition temperature  $T_{\text{trans}}$  under a constant strain  $\epsilon_m$  to a temperature  $T_{\text{low}}$ , thus fixing the temporary shape. Retracting the clamps of the tensile tester to the original distance of 0% strain causes the sample to bend. After heating the sample up to  $T_{\text{high}} > T_{\text{trans}}$ , it contracts and the permanent shape is recovered. The cycle then begins again.

The result of such a measurement is usually presented in a  $\epsilon$ - $\sigma$  curve (Figure 6a;  $\sigma$  = tensile stress). This is the reason for this test protocol being called a "two-dimensional measurement". Figure 6 represents schematic curves. Different effects can result in changes to the curve, particularly when the stretched sample is cooled down (position ② in Figure 6a). Among others, the following effects play a role in these changes: differences in the expansion coefficient of the stretched sample at temperatures above and below  $T_{\text{trans}}$  as a result of entropy elasticity (see Section 2.1.3, Figure 4), as well as volume changes arising from crystallization in the case of  $T_{\text{trans}}$  being a melting point.

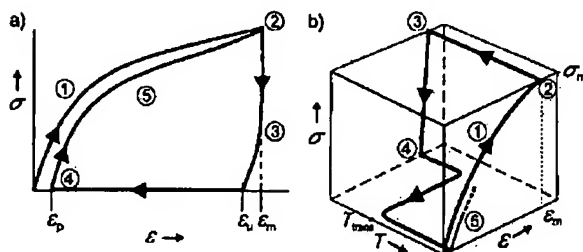


Figure 6. Schematic representation of the results of the cyclic thermomechanical investigations for two different tests: a)  $\epsilon$ - $\sigma$  diagram: ①—stretching to  $\epsilon_m$  at  $T_{\text{high}}$ ; ②—cooling to  $T_{\text{low}}$  while  $\epsilon_m$  is kept constant; ③—clamp distance is driven back to original distance; ④—at  $\epsilon = 0\%$  heating up to  $T_{\text{high}}$ ; ⑤—start of the second cycle. b)  $\epsilon$ - $T$ - $\sigma$  diagram: ①—stretching to  $\epsilon_m$  at  $T_{\text{high}}$ ; ②—cooling down to  $T_{\text{low}}$  with cooling rate  $k_{\text{cool}} = dT/dt$  while  $\sigma_m$  is kept constant; ③—clamp distance is reduced until the stress-free state  $\sigma = 0$  MPa is reached; ④—heating up to  $T_{\text{high}}$  with a heating rate  $k_{\text{heat}} = dT/dt$  at  $\sigma = 0$  MPa; ⑤—start of the second cycle.

In addition to the elastic modulus  $E(T_{\text{high}})$  at  $T_{\text{high}}$ , which can be determined from the initial slope in the measurement range ① (Figure 6a), the elastic modulus of the stretched sample at  $T_{\text{low}}$  can also be determined from the slope of the curve at ③ (Figure 6a). The important quantities to be determined for describing the shape-memory properties of the material at a strain  $\epsilon_m$  are the strain recovery rate  $R_r$  and the strain fixity rate  $R_f$ . Both can be determined according to

equations (4), (5), and (6) from cyclic, thermomechanical measurements.

The strain recovery rate  $R_r$  quantifies the ability of the material to memorize its permanent shape and is a measure of how far a strain that was applied in the course of the programming  $\epsilon_m - \epsilon_p(N-1)$  is recovered in the following shape-memory transition. For this purpose the strain that occurs upon programming in the  $N$ th cycle  $\epsilon_m - \epsilon_p(N-1)$  is compared to the change in strain that occurs with the shape-memory effect  $\epsilon_m - \epsilon_p(N)$  [Eq. (4)].  $\epsilon_p(N-1)$  and  $\epsilon_p(N)$

$$R_r(N) = \frac{\epsilon_m - \epsilon_p(N)}{\epsilon_m - \epsilon_p(N-1)} \quad (4)$$

represent the strain of the sample in two successively passed cycles in the stress-free state before yield stress is applied. The total strain recovery rate  $R_{r,\text{tot}}$  is defined as the strain recovery after  $N$  passed cycles based on the original shape of the sample [Eq. (5)]. The strain fixity rate  $R_f$  describes the ability

$$R_{r,\text{tot}}(N) = \frac{\epsilon_m - \epsilon_p(N)}{\epsilon_m} \quad (5)$$

of the switching segment to fix the mechanical deformation which has been applied during the programming process. It describes how exactly the sample can be fixed in the stretched shape after a deformation to  $\epsilon_m$ . The resulting temporary shape always differs from the shape achieved by deformation. The strain fixity rate  $R_f$  is given by the ratio of the strain in the stress-free state after the retraction of the tensile stress in the  $N$ th cycle  $\epsilon_p(N)$  and the maximum strain  $\epsilon_m$  [Eq. (6)].<sup>[1]</sup>

$$R_f(N) = \frac{\epsilon_p(N)}{\epsilon_m} \quad (6)$$

As indicated in Figure 6, the first few cycles can differ from each other. The curves become more similar with an increasing number of cycles. The process of deformation and recovery of the permanent shape becomes highly reproducible. The changes in the first few cycles are attributed to the history of the sample, thus, processing and storage play an important role. During the first cycles a reorganization of the polymer on the molecular scale takes place which involves deformation in a certain direction. Single polymer chains arrange in a more favorable way in regard to the direction of deformation. Covalent bonds may be broken during this process.

An important variable that can not be determined by a two-dimensional measurement is  $T_{\text{trans}}$ . In this respect, the three-dimensional test record is interesting, and is shown schematically in Figure 6b. In contrast to the two-dimensional measurement, the sample is cooled down in a controlled way at a strain of  $\epsilon_m$  and a constant tensile stress  $\sigma_m$ . The change in strain in this region is influenced by the temperature dependence of the coefficient of thermal expansion of the stretched polymer (see Section 2.1.3) and volume effects based on the thermal transition at  $T_{\text{trans}}$  (for example, a crystallization process). Having reached  $T_{\text{low}}$ , the strain is driven back until a stress-free state is reached. The sample is then heated up to  $T_{\text{high}}$  in a controlled way. In the course of this experiment the tensile stress is kept constant at 0 MPa, which

means that the clamps follow the movement of the test piece. The mechanical movement occurring in the course of the shape-memory effect is recorded as a function of the temperature. Both the temperature interval as well as  $T_{\text{trans}}$  in which the shape-memory effect takes place can be determined from the interpretation of the  $\epsilon$ - $T$  plane of the  $\epsilon$ - $T$ - $\sigma$  diagram.

### 2.3.2. Bending Test for the Determination of the Shape-Memory Effect

In the course of the bending test a sample is bent at a given angle  $\theta_i$  at a temperature above the switching transition and is kept in this shape. The so-deformed sample is cooled down to a temperature  $T_{\text{low}} < T_{\text{trans}}$  and the deforming stress is released. Finally, the sample is heated up to the measuring temperature  $T_{\text{high}} > T_{\text{trans}}$  and the recovery of the permanent shape is recorded. The deformation angle  $\theta_i$  varies as a function of time. The recovery rate  $R_\theta$  is calculated from the ratio of the different angles before and after recovery  $\theta_i$  and the deformation angle  $\theta_i$  in the temporary shape [Eq. (7)].<sup>[18, 19]</sup>

$$R_\theta = \frac{(\theta_i - \theta_f)}{\theta_i} \quad (7)$$

### 2.3.3. Shrinkage Determination of Heat-Shrinkable Products

The test samples stretched at room temperature are kept under a constant stress of about 0.2 MPa and heated above  $T_{\text{trans}}$ . In the case of polyethylene cross-linked by means of ionizing rays, the material is heated up above the melting point of the PE crystallites. The shrinkage is then given by the ratio [Eq. (8)], where  $\lambda = l_{\text{st}}/l_0$ ,  $l_{\text{st}}$  is the length of the stretched sample, and  $l_i$  the length of the sample after the shrinkage process. Partly, instead of the original length of the sample  $l_0$ , the stretching ratio  $\lambda$ , the ratio of the length of the stretched sample  $l_{\text{st}}$  and  $l_0$ , is used. The shrinkage process depends on the temperature  $T_{\text{high}}$ . Therefore, the shrinkage  $l_i(t)$  is often determined as a function of time for a given shrinkage temperature  $T_{\text{high}}$ .<sup>[49, 50]</sup>

$$\text{Heat shrinkage [\%]} = \frac{l_{\text{st}} - l_i}{l_{\text{st}} - l_0} 100 = \frac{l_{\text{st}} - l_i}{l_{\text{st}} (1 - \lambda^{-1})} 100 \quad (8)$$

## 2.4. Physically Cross-Linked Shape-Memory Polymers

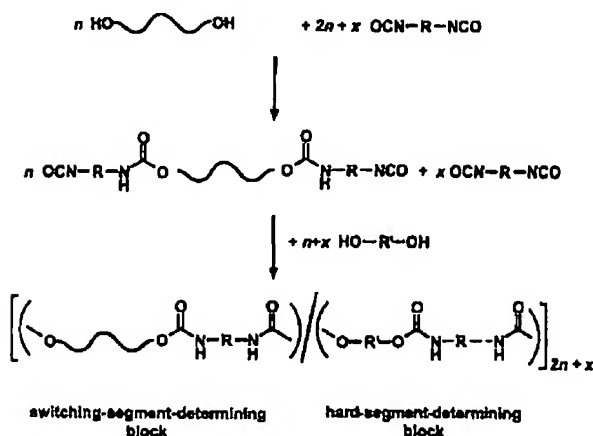
### 2.4.1. Linear Block Copolymers

In this section shape-memory polymers are presented that form part of the class of linear block copolymers. The mechanism of the thermally induced shape-memory effect of these materials is based on the formation of a phase-segregated morphology, which has been described in Section 2.2, with one phase acting as a molecular switch. Through the formation of physical netpoints, the phase with the highest thermal transition  $T_{\text{perm}}$  on the one hand provides the mechanical strength of the material, especially at  $T < T_{\text{perm}}$ , and on the other hand is responsible for the fixation that determines the permanent shape. The materials are divided into two categories according to the thermal transition of the particular switching segment on which the shape-memory effect is based. Either the transition temperature  $T_{\text{trans}}$  is a melting temperature  $T_m$  or a glass transition temperature  $T_g$ . In the case of a melting temperature, one observes a relatively sharp transition in most cases while glass transitions always extend over a broad temperature range. Mixed glass transition temperatures  $T_{g\text{mix}}$  between the glass transition of the hard-segment- and the switching-segment-determining blocks may occur in the cases where there is no sufficient phase separation between the hard-segment-determining block (block A) and the switching-segment-determining block (block B). Mixed glass transition temperatures can also act as switching transitions for the thermally induced shape-memory effect. Table 1 gives an overview of the various possible combinations of hard-segment- and switching-segment-determining blocks in linear, thermoplastic shape-memory polymers.

All the linear polyurethane systems presented in the following paragraph are synthesized according to the prepolymer method. Thermoplastic polyurethane elastomers are produced on an industrial scale by means of this technique. In this process, isocyanate-terminated pre-polymers are obtained by reaction of difunctional, hydroxy-terminated oligoesters and -ethers with an excess of a low molecular weight diisocyanate (Scheme 1, 1st reaction step). Low molecular weight diols and diamines are added as so called chain extenders to further couple these prepolymers. Linear, phase-segregated polyurethane- or polyurethane-urea block copolymers are obtained in this way (Scheme 1, 2nd reaction step). Each polymer chain contains segments of high polarity composed of urethane and urea bonds that are linked through

Table 1. Possible combinations of hard-segment- (block A) and switching-segment-determining blocks (block B) in linear, thermoplastic block copolymers with thermally induced shape-memory effects. In the block polymers in category 1 the permanent shape is determined by the thermal transition at melting ( $T_{\text{perm}} = T_m$  A), in category 2 at the glass transition ( $T_{\text{perm}} = T_g$  A) of the hard-segment-determining block.

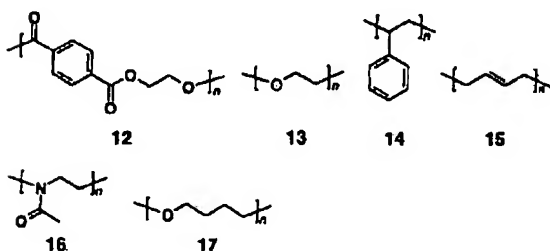
Category	Block A		Block B		Phase-segregated block copolymers	
	highest thermal transition	2nd thermal transition	highest thermal transition	2nd thermal transition	$T_{\text{perm}}$	possible switching transitions $T_{\text{trans}}$
1.1	$T_{mA}$	$T_{gA}$	$T_{mB}$	$T_{gB}$	$T_{mA}$	$T_{mB}, T_{gA}, T_{gB}$
1.2	$T_{mA}$	$T_{gA}$	$T_{mB}$	$T_{gB}$	$T_{mA}$	$T_{mB}, T_{g\text{mix}}$
1.3	$T_{mA}$	$T_{gA}$	$T_{gB}$		$T_{mA}$	$T_{gA}, T_{gB}$
1.4	$T_{mA}$	$T_{gA}$	$T_{gB}$		$T_{mA}$	$T_{g\text{mix}}$
2.1	$T_{gA}$		$T_{mB}$	$T_{gB}$	$T_{gA}$	$T_{mB}, T_{gB}$
2.2	$T_{gA}$		$T_{mB}$	$T_{gB}$	$T_{gA}$	$T_{mB}, T_{g\text{mix}}$
2.3	$T_{gA}$		$T_{gB}$		$T_{gA}$	$T_{gB}$



Scheme 1. Prepolymer method for the synthesis of thermoplastic polyurethanes. R and R' are short chain groups with two free valences.

chain-extender molecules. As a consequence of their high intermolecular interaction, they form the so called hard segments. Strictly speaking, they represent the hard-segment-forming phase that is embedded in an amorphous elastic matrix. This amorphous matrix, with its low glass transition temperature lying far below the normal operating temperature, forms the so called soft segment. In the case of polyurethanes with shape-memory effects, this segment serves as a switching segment. For this purpose it is modified in such way that the thermal transition is located in a temperature range relevant for the respective application. Hard segment "clusters" with dimensions under 1  $\mu\text{m}$  are formed by the phase-separation process that occurs. These clusters have high  $T_g$  or  $T_m$  values and act as multifunctional physical netpoints. These so-called plastic domains act as a reinforcing filler. Their ability to deflect mechanical energy by deformation enables the growth of microcracks to be prevented. They also impart cross-breaking strength and impact strength to the material.<sup>[51]</sup>

In the following paragraph polymer systems are introduced whose shape-memory effect can be triggered by the transition of a melting point. Shape-memory polymers with  $T_{\text{trans}} = T_m$  are represented by polyurethanes, polyurethanes with ionic or mesogenic components, block copolymers consisting of poly(ethyleneterephthalate) (12, PET) and poly(ethyleneoxide) (13, PEO), block copolymers containing polystyrene (14) and poly(1,4-butadiene) (15), and an ABA triblock copolymer made from poly(2-methyl-2-oxazoline) (16, A block) and poly(tetrahydrofuran) 17 (B block). Polyurethane systems with



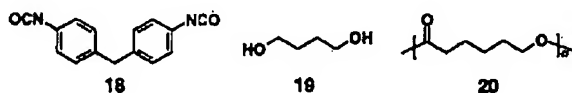
$T_{\text{trans}} = T_g$  are then introduced. Table 2 gives an overview of the chemical composition of the linear block copolymers and their respective transition temperatures that resulted in switching transitions, as well as the variability in the switching temperatures.

The thermal transitions of the pure polymer blocks of those shape-memory materials mentioned in paragraph 2.4.1 are listed in Table 3.

#### 2.4.1.1. Multiblock Copolymers with $T_{\text{trans}} = T_m$

##### Polyurethanes with a Poly( $\epsilon$ -caprolactone) Switching Segment

Kim and co-workers synthesized polyesterurethanes (PEUs, Table 2, first entry) with a hard-segment-determining block of methylenebis(4-phenylisocyanate) (18, MDI) and 1,4-butanediol (19) by using the pre-polymer method.<sup>[13, 14, 52]</sup> The highest thermal transition  $T_{\text{perm}}$  corresponding to the



melting temperature of the hard-segment-determining blocks is found in the range between 200 and 240 °C. Poly( $\epsilon$ -caprolactone)diols with a number-average molecular weight ( $M_n$ ) between 1600 and 8000 form the switching segments. The switching temperature for the shape-memory effect can vary between 44 and 55 °C depending on the weight fraction of the switching segments (variation between 50 and 90 wt %) and the molecular weight of the used poly( $\epsilon$ -caprolactone)diols. The crystallinity of the switching segment blocks determined by comparison of the partial melt enthalpies with the melt enthalpy of 100 % crystalline poly( $\epsilon$ -caprolactone) (20) becomes higher as the weight fraction and the molecular weight of the poly( $\epsilon$ -caprolactone)diols used increases. Hence, the crystallization of the poly( $\epsilon$ -caprolactone) segments is hindered by incorporating them into the multiblock copolymers. The crystallinity observed is between 10 and 40 %. No crystallization can be observed when the poly( $\epsilon$ -caprolactone)diol has a number-average molecular weight below 2000, presumably, because of the low degree of phase separation. In cyclic thermomechanical measurements, an increase of the initial slope with the number of cycles is found. A behavior which is named "cyclic hardening" can be observed during the initial four to five cycles. This effect is caused by a relaxation of the material in the stretched state which results in an increasing orientation and crystallization of the chains. As a consequence, the resistance of the material against the strain grows with the number of cycles. The materials reach constant strain recovery rates after the third cycle. Polyurethanes formed from a high molecular weight poly( $\epsilon$ -caprolactone) and a high weight fraction of hard-segment-determining blocks show the best shape-memory properties: the strain recovery rate increases up to 98 % with strains  $\epsilon_m$  of 80 %. Moreover, the shape-memory properties are strongly influenced by the degree of strain applied: the strain recovery rates reached decrease with applied strains of

Table 2. Overview of linear, thermoplastic block copolymers with thermally induced shape-memory effects.

Category according to Table 1	Hard-segment-forming phase	Switching-segment-forming phase	$T_{\text{DM}}$ [°C]	Ref.
<i>Multiblock copolymers with <math>T_{\text{trans}} = T_m</math></i>				
1.1	MDI/1,4-butanediol	poly( $\epsilon$ -caprolactone) ( $M_n = 1600, 2000, 4000, 5000, 7000, \text{ and } 8000$ )	$T_m$ of poly( $\epsilon$ -caprolactone) crystallites: 44–55	[13, 14, 52]
1.1	MDI/1,4-butanediol dimethylolpropionic acid	poly( $\epsilon$ -caprolactone) ( $M_n = 2000, 4000, \text{ and } 8000$ )	$T_m$ of poly( $\epsilon$ -caprolactone) crystallites: 45–55	[17]
1.2 (mesogenic segments cause further transitions)	MDI/BEBP or BHBP	poly( $\epsilon$ -caprolactone) ( $M_n = 4000$ )	$T_m$ of poly( $\epsilon$ -caprolactone) crystallites: 41–50	[53]
1.2 (mesogenic segments cause further transitions)	HDI/4,4'-dihydroxybiphenyl	poly( $\epsilon$ -caprolactone) ( $M_n = 4000$ )	$T_m$ of poly( $\epsilon$ -caprolactone) crystallites: 38–59	[54]
1.2 (mixed $T_g$ at $-25$ – $15$ °C)	poly(ethylene terephthalate)	poly(ethylene oxide) ( $M_n = 4000, 6000, 10000$ )	$T_m$ of poly(ethylene oxide) crystallites: 40–60	[15, 16, 55]
2.1	PS (14)	poly(1,4-butadiene) (15)	$T_m$ of polybutadiene crystallites: 45–65	[56, 95]
2.1 (ABA triblock copolymer)	poly(2-methyl-2-oxazoline)	poly(tetrahydrofuran) ( $M_n = 4100$ – $18800$ )	$T_m$ of poly(tetrahydrofuran) crystallites: 20–40	[57]
<i>Multiblock copolymers with <math>T_{\text{trans}} = T_g</math></i>				
1.1 (separate $T_g$ values for poly(tetrahydrofuran) segments with $M_n = 1000, 2000, 2900$ )	MDI/1,4-butanediol	poly(tetrahydrofuran) ( $M_n = 250, 650, 1000, 2000, 2900$ )	$T_g$ of poly(tetrahydrofuran) segments or mixed $T_g$ : $-56$ – $54$	[18, 19]
1.2 (mixed $T_g$ for poly(tetrahydrofuran) segments with $M_n = 250, 650$ )				
1.3	MDI/1,4-butanediol	poly(ethylene adipate) ( $M_n = 300, 600, 1000, 2000$ )	$T_g$ of poly(ethylene adipate) segments: $-5$ – $48$	[11]
1.2–1.4	2,4-TDI or MDI	poly(propylene oxide) ( $M_n = 400, 700, 1000$ )	$T_g$ : $-45$ – $48$	[58, 59]
	carbodiimide-modified diisocyanates (MDI and HDI)	poly(butylene adipate) ( $M_n = 600, 1000, 2000$ )		
	ethylene glycol or bis(2-hydroxyethyl)hydroquinone	poly(tetrahydrofuran) ( $M_n = 400, 650, 700, 850, 1000$ )		
	combination of (2,2'-bis(4-hydroxyphenyl)-propane (bisphenol A) and ethylene oxide	combination of (2,2'-bis(4-hydroxyphenyl)-propane (bisphenol A) and propylene oxide ( $M_n = 800$ )		
		poly(ethylene oxide) ( $M_n = 600$ )		

250 % from rates of more than 90 % to rates of 80 %. Besides the crystallinity of the switching segments, the decisive factors that influence the recovery properties are the formation and stability of the hard-segment-forming domains, especially in the temperature range above the melting temperature of the switching-segment crystallites. Above a lower limit of the hard-segment-determining blocks of 10 wt %, the hard-segment domains are no longer sufficiently pronounced to function efficiently as physical cross-links. A slight increase in the switching temperature can be observed during the initial three cycles. This behavior is interpreted as the destruction of weak netpoints followed by an increasing formation of an ideal elastic network. Tables 4 and 5 show values determined for the shape recovery and shape fixity rates. The samples were stretched at room temperature after a thermal pretreatment at 80 °C.

#### Incorporation of Ionic Components into the Hard-Segment-Forming Phase

Several investigations have dealt with the question as to whether the incorporation of ionic or mesogenic moieties into the hard-segment-forming phase can influence the mechan-

ical and shape-memory properties through the introduction of additional intermolecular interactions by possibly enhancing the degree of phase separation. For this purpose, polyester urethanes have been synthesized by the pre-polymer method using MDI and 1,4-butanediol as the hard-segment-determining block. Half of the chain-extending 1,4-butanediol in the hard-segment-forming phase was substituted by 2,2-bis(hydroxymethyl)propionic acid (21) so as to introduce additional intermolecular interactions.<sup>[17]</sup> Poly( $\epsilon$ -caprolactone)diols with number-average molecular weights between 2000 and 8000 were used as the switching-segment-forming phase. The weight fraction of the switching segment was around 70 wt % for materials based on poly( $\epsilon$ -caprolactone)diols with number-average molecular weights between 2000 and 8000 and varied between 55 and 90 wt % for poly( $\epsilon$ -caprolactone)diol with a molecular weight of 4000. The switching temperatures for the shape-memory effect were between 44 and 55 °C. A hard-segment phase additionally stabilized by ionic interactions can be formed by neutralization of the propionic acid moieties with triethylamine. These multiblock copolymers having polyelectrolyte character are so called "ionomers". As a result of their additional Coulomb

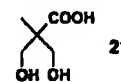


Table 3. Thermal properties of the pure polymer blocks.

Polymer block	Block type	$T_m$ [°C]	$T_g$ [°C]
MDI/1,4-butanediol	A	200–240 <sup>[60]</sup> 193–232 <sup>[61]</sup>	125 <sup>[62]</sup> 100 <sup>[63]</sup>
poly( $\epsilon$ -caprolactone)	B	$M_n = 1600$ : 46.3 $M_n = 4000$ : 53.5 $M_n = 7000$ : 55.9 <sup>[64]</sup> $M_n > 10000$ (semicrystalline): 59–64 <sup>[63, 65]</sup>	–60 <sup>[67]</sup>
poly(tetrahydrofuran)	B	$M_n = 250$ : –7.9 $M_n = 250$ : –95 <sup>[72]</sup> $M_n = 650$ : 20.2 $M_n = 1000$ : 23.6 $M_n = 2000$ : 27.7 $M_n = 2900$ : 45.8 <sup>[68]</sup> 57 <sup>[69]</sup>	–84 °C <sup>[71]</sup> –46 <sup>[72]</sup>
poly(ethylene adipate)	B		81 (semicrystalline) <sup>[73]</sup>
poly(ethylene terephthalate)	A	260 (semicrystalline) <sup>[74]</sup> 280 (semicrystalline, equilibrium) <sup>[74]</sup>	125 (semicrystalline and oriented) <sup>[74]</sup>
poly(ethylene oxide)	B	$M_n = 1400$ –1600: 45–50 $M_n = 1900$ –2200: 50–52 $M_n = 3500$ –4000: 59–61 $M_n = 5000$ –7000: 60–63 $M_n = 8500$ –11 500: 63–65 <sup>[77]</sup> 69 <sup>[74]</sup>	–67 <sup>[76]</sup> 100 (amorphous) <sup>[82]</sup> 90 <sup>[83]</sup>
PS(14)	A	270 <sup>[80]</sup> 240 <sup>[81]</sup>	–107 <sup>[86]</sup>
poly(1,4-butadiene) (15)	B	97 (modification I) 145 (modification II) <sup>[84, 85]</sup>	
Polyethylene	A	134 (90 % crystalline, linear PE) 115 (60 % crystalline; LDPE) <sup>[87]</sup>	–125 to –120 ( $\gamma$ ) –80 to –40 ( $\beta$ ) <sup>[88]</sup>
poly(vinyl acetate)	B		31 <sup>[89]</sup>
polyamide-6 (nylon-6)	A	215–220 <sup>[90]</sup> 223 <sup>[91]</sup>	40 <sup>[92]</sup>
poly(2-methyl-2-oxazoline)	A		480 <sup>[93]</sup>

Table 4. Dependence of the strain recovery rate after the first cycle ( $R_f(1)$  in %) at  $\epsilon_m = 80\%$  on the switching segment content SC [wt %] for different molecular weights  $M_n$  of the used poly( $\epsilon$ -caprolactone)diols.<sup>[14]</sup>

$M_n$	SC	$R_f(1)$	$M_n$	SC	$R_f(1)$
4000	81	98	7000	92	60
5000	89	50	7000	88	93
5000	84	96	7000	85	95
5000	80	98	7000	81	98

Table 5. Dependence of the strain recovery rate ( $R_f$ ) and strain fixity rate ( $R_f$ ) after the first and fourth cycle on the switching segment content SC [wt %] and the strain  $\epsilon_m$  for different molecular weights  $M_n$  of the poly( $\epsilon$ -caprolactone)diols used.<sup>[15]</sup>

$M_n$	SC	$\epsilon_m$	$R_f(1)$ [%]	$R_f(4)$ [%]	$R_f(1)$ [%]	$R_f(4)$ [%]
2000	70	200	48	20	95	98
2000	55	200	73	65	58	60
4000	75	600	75	60	85	90
4000	70	200	82	73	92	95
8000	55	200	62	52	88	90

interactions, they exhibit a higher elastic modulus and higher mechanical strength than the systems containing uncharged hard segment blocks. The transition from the uncharged multiblock copolymers to ionomers results in an increase in the elastic moduli to between 24 and 34 % at 25 °C, depending on the molecular weight and the weight fraction of the poly( $\epsilon$ -caprolactone)diols used. An increase in the elastic moduli between 38 and 156 % is observed at 65 °C. In addition, an

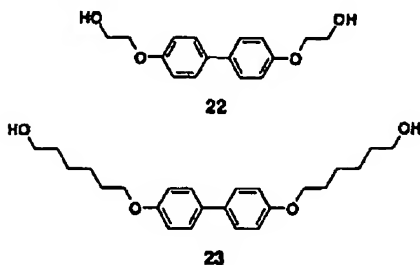
increasing hard-segment content increases the mechanical stability of the materials. The charged systems show up to approximately 10 % higher strain recovery rates and equal strain fixity rates relative to the uncharged systems. Table 6 displays the strain fixity and strain recovery rates for two materials with and without ionomer, both based on poly( $\epsilon$ -caprolactone)diol with a number-average molecular weight of 4000 and a poly( $\epsilon$ -caprolactone) content of 70 wt %.

Table 6. Comparison of strain recovery rate ( $R_f$ ) and strain fixity rate ( $R_f$ ) at  $\epsilon_m = 200\%$  and a switching segment content of 70 wt % for ionomers and the corresponding non-ionomers.<sup>[17]</sup>

	$R_f(1)$ [%]	$R_f(4)$ [%]	$R_f(1)$ [%]	$R_f(4)$ [%]
ionomer (charged)	66	45	95	95
non-ionomer (uncharged)	62	35	95	95

#### Incorporation of Mesogenic Components into the Hard-Segment-Forming Phase

In the case of the incorporation of mesogenic diols such as 4,4'-bis(2-hydroxyethoxy)biphenyl (22, BEBP) or 4,4'-bis(2-hydroxyhexoxy)biphenyl (23, BHBP) into the hard-segment-determining blocks based on MDI, an increased solubility of these blocks in the switching segment made of poly( $\epsilon$ -caprolactone) ( $M_n = 4000$ ) is observed.<sup>[53]</sup> As a consequence, a mixed  $T_g$  value of the hard-segment- and switching-segment-forming phase occurs. The strain-induced fixa-



tion observed is attributed to crystallization of the switching-segment blocks. An increase in the strain fixity rate of more than 20% is observed in the case of the polymers with added BEBP with a switching-segment content increasing from 60 to 80 wt% and a strain  $\epsilon_m$  value of 100%. Materials with added BHBP show an increase in the strain fixity rate of 5 to 10% with a strain  $\epsilon_m$  of 100 to 300%. Table 7 shows an overview of the recorded shape-memory properties. The strain recovery rates observed at a strain  $\epsilon_m$  of 100% correspond to those with a hard-segment-forming phase containing MDI/1,4-butanediol.

Table 7. Dependence of the strain recovery rate ( $R_r(4)$ ) and strain fixity rate ( $R_f(4)$ ) of multiblock copolymers with a hard-segment-forming phase of MDI/1,4-butanediol after the fourth cycle on the switching segment content SC [wt %], the strain  $\epsilon_m$ , and the added mesogenic diols.<sup>[6]</sup>

Additive	SC	$\epsilon_m$ [%]	$R_r(4)$ [%]	$R_f(4)$ [%]
BEBP	80	100	80	98
BEBP	71	100	80	95
BEBP	57	100	85	75
BHBP	80	100	85	85
BHBP	70	100	80	80
BHBP	59	100	85	80
BHBP	80	300	68	95
BHBP	70	300	73	90
BHBP	59	300	63	85

[a] The values are calculated from Figures 2–4 in ref. [53].

#### Block Copolymers Made of Polyethylene Terephthalate (12) and Polyethylene Oxide (13)

A further example of shape-memory polymers with  $T_{\text{trans}} = T_m$  are linear, phase-separated block copolymers with a hard-segment-forming phase based on PET and switching-segment blocks of PEO.<sup>[15, 16, 35, 94]</sup> The highest thermal transition  $T_{\text{perm}}$  is the melting point of the PET blocks at 260°C. The thermally induced shape-memory effect is triggered by the melting temperature of the PEO crystallites and can be varied between 40 and 60°C depending on the molecular mass of the PEO blocks or on the PET content (see Table 2).

The crystalline fraction of the switching segments increases as the molecular weight of the PEO blocks grows. Simultaneously, the melting temperature of the PEO blocks increases as their molecular weight increases. The crystallization of the PEO blocks is more and more hindered as the weight fraction of PET increases. As a consequence, the melting temperature of the switching segment with the same molecular weight decreases in the case of a polymer with an increased content of hard-segment-determining PET blocks. Stretching a sample

at a temperature near the melting temperature of the PEO segments results in the crystallites of the PEO segments becoming parallelly orientated. They change their shape from spherulitic to fibril-like structures. If these structures are too well developed they hinder the recovery process. This is why a change in the strain recovery rate as a function of the applied strain  $\epsilon_m$  is observed depending on the composition of the copolymer or on the developed morphology. To investigate the strain recovery rate the samples were stretched above the melting point of the PEO crystallites at 58°C, cooled down, and heated up again with a heating rate of 1 K min<sup>-1</sup>. The shrinkage observed upon heating increases with an increasing molecular weight of the PEO segments up to strains  $\epsilon_m$  (up to 100%). After reaching a maximum at a strain of around 150%, the observed shrinkage decreases again. The series of block copolymers investigated here shows improved strain recovery rates if the weight fraction of PET increases. This behavior is explained with the formation of more stable physical bonds in the better aggregated PET blocks. The temperature at which the highest recovery rate can be observed is the so-called recovery temperature  $T_r$ . This temperature is found in the range of the melting temperature of the PEO switching segment. Tables 8 and 9 show typical shape-memory properties of PET/PEO block copolymers.

Table 8. Dependence of the strain recovery rate after the first cycle ( $R_r(1)$ ) and the recovery temperature  $T_r$  on the switching segment content SC [wt %] and the strain  $\epsilon_m$  for different molecular weight  $M_n$  poly(ethylene oxide)diols taken from Table 2 in ref. [15].

$M_n$	SC	$T_r$ [°C]	$R_r(1)$ [%]	$\epsilon_m$ [%]
2000	73	—	—	—
4000	68	43.0	89.8	85
6000	79	48.0	98.7	120
6000	74	47.5	99.1	120
6000	68	46.8	98.9	120
10000	83	54.5	99.5	150
10000	78	53.4	99.7	150

Table 9. Dependence of the strain recovery rate after the first cycle  $R_r(1)$  (in %) at  $\epsilon_m = 180\%$  and  $T_m$  [°C] on the switching segment content SC [wt %] for different molecular weight  $M_n$  poly(ethylene oxide)diols in Table 2 in ref. [16].

$M_n$	SC	$T_m$	$R_r(1)$	$M_n$	SC	$T_m$	$R_r(1)$
4000	72	45.2	84	6000	74	46.5	92
4000	68	43.9	85	10000	83	54.5	93
6000	79	47.3	90	10000	78	52.7	95

#### Block Copolymers Made of Polystyrene (14) and Poly(1,4-butadiene) (15)

The poly(1,4-butadiene) blocks in phase-segregated block copolymers consisting of 34 wt% PS and 66 wt% poly(1,4-butadiene) are found to be semicrystalline with a high *trans* ratio.<sup>[5a, 95]</sup> The melting temperature of the poly(1,4-butadiene) crystallites represents the switching temperature for the thermally induced shape-memory effect. The glass transition of the polystyrene is the highest thermal transition  $T_{\text{perm}}$  and is found at 90°C. Thus, polystyrene supplies the hard-

segment-determining blocks. The high glass transition temperature of the polystyrene blocks hinders the polybutadiene chains from slipping off each other upon stretching. The elastic properties, which are not only responsible for the elastic strain but also for the recovery because of the material's entropy relaxation, are attributed to the amorphous areas of the polybutadiene phase. For a material with a poly(1,4-butadiene) content of 86 mol % and a weight-average molecular weight of 70 000, the formation of two crystal modifications in the polybutadiene blocks is reported. One of the observed crystal modifications is stable at room temperature. First, the low temperature modification converts into the high temperature modification upon heating up to temperatures higher than 45°C. Only if a temperature of 65°C is exceeded does the poly(1,4-butadiene) reach a completely molten, amorphous state. A reversible solid-state transformation is possible between the two crystal modifications. Whereas, a melting point usually guarantees a sharp transition, here, the existence of the two different crystal modifications does not allow an exact tuning of the switching temperature. A high strain recovery rate in the range of 80 % is observed ( $T = 80^\circ\text{C}$ ) upon application of a maximum strain  $\epsilon_m$  in the range of 100 %.  $R_s$  still reaches values of around 60 % at a maximum strain  $\epsilon_m$  of more than 400 %. The appearance of the shape-memory effect is explained by the formation of oriented crystallites upon application of high elongations of up to 600 %. These oriented crystallites form a fibril-like structure with high regularity over large distances. The single fibrils are linked through amorphous 1,4-polybutadiene chains that are anchored in several crystallites at the same time. The highly ordered morphology described remains stable even after heating above 80°C.

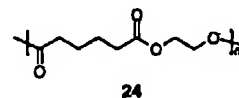
*ABA Triblock Copolymers Made from Poly(tetrahydrofuran) (17) and Poly(2-methyl-2-oxazoline) (16)*

ABA triblock copolymers with a central poly(tetrahydrofuran) block (B block) with number-average molecular weights between 4100 and 18 800 and equipped with terminal poly(2-methyl-2-oxazoline) blocks (A block) with molecular weights of 1500 are obtained by cationic ring-opening polymerization.<sup>[57]</sup> The A blocks exhibit glass transition temperatures around 80°C and represent the hard-segment-forming phase. The poly(tetrahydrofuran) blocks are semi-crystalline and exhibit a melting temperature between 20 and 40°C, depending on their molecular weight. These melting temperatures are used as switching temperatures for a thermally induced shape-memory effect. As the thermal data of the two different segments do not differ significantly from the values of the respective homopolymers, one can assume that the material shows microphase separation. The materials with poly(tetrahydrofuran) blocks having a molecular weight greater than 13 000 exhibit very good mechanical strength at room temperature. In contrast to pure poly(tetrahydrofuran), the block copolymer materials show elastic properties and incomplete softening even above the melting temperature of the poly(tetrahydrofuran) segments. This observation is interpreted as the formation of a network with physical cross-links by the poly(2-methyl-2-oxazoline) blocks. These

blocks solidify below 80°C to form a glass. If a sample with a number-average molecular weight of the central poly(tetrahydrofuran) block of 19 000 is stretched to 250 % elongation at 22°C, half the elongation will be kept after releasing the external stretching force. A nearly complete recovery takes place upon heating the sample to 40°C.

*2.4.1.2. Multiblock Copolymers with  $T_{\text{trans}} = T_g$*

In phase-segregated block copolymers a glass transition can also be used as the switching transition for the shape-memory effect. A prerequisite is a glass transition that takes place within a narrow temperature range and above the usual operating temperature of this material. In the following paragraph, polymer systems are introduced whose shape-memory effect can be triggered by using a glass transition. All examples are polyurethane systems, in which the hard-segment-forming phase is synthesized from MDI/1,4-butanediol. The switching segment blocks are mostly polyethers such as poly(tetrahydrofuran) but also polyesters such as poly(ethylene adipate) (24) are used. In the case of an almost complete phase separation, the glass transition temperature used as the switching transition can origin from the pure switching-segment blocks. In the case of less-separated phases, which can typically be found for short switching-segment blocks, a mixed  $T_g$  value from the glass transition temperatures of the hard-segment-forming and the switching-segment-forming phase can occur. This mixed  $T_g$  value can be found between the glass transition temperatures of the pure hard-segment- and switching-segment-determining blocks.



An example of materials with a mixed  $T_g$  value are the systems with poly(tetrahydrofuran) switching-segment blocks having number-average molecular weights of 250 and 650 that have been provided with a hard-segment-forming phase from MDI and 1,4-butanediol by using the pre-polymer method.<sup>[18, 19]</sup> The highest thermal transition  $T_{\text{perm}}$  corresponding to the melting temperature of the hard-segment-forming phase can be found between 200 and 240°C. The phase-segregated block copolymers containing a switching segment with a molecular weight of  $M_n = 250$  exhibit a  $T_g$  value in the range between 16 and 54°C, depending on the hard-segment content (hard-segment content between 57 and 95 wt %), a  $T_g$  value between -13 and 38°C for a switching segment with a molecular weight  $M_n = 650$  (hard segment content between 32 and 87 wt %), and a  $T_g$  value between -36 and 22°C for a switching segment with a molecular weight of  $M_n = 1000$  (content of hard segment determining blocks between 23 and 81 wt %). A mixed  $T_g$  value can not be observed if poly(tetrahydrofurans) with a molecular weight of 2000 or 2900 are used because of the good separation of the different blocks. Here, the occurring glass transition temperatures of the poly(tetrahydrofuran) blocks are also dependent on the hard-segment content because the hard segments restrict the mobility of the switching-segment chains.

The shape-memory behavior is determined by means of a bending test (see Section 2.3.2). In the course of the bending

test, the sample is bent at a certain angle  $\theta$ , at 80 °C and kept in this deformation. The deformed sample is quickly cooled down to -20 °C and the external force is released. Finally, the sample is brought to the test temperature and its recovery to the original angle is recorded. The deformation recovery rate is calculated from Equation (7). The  $T_g$  value increases with increasing amounts of the hard-segment-determining blocks. As a consequence, the temperature at which the shape-memory effect is triggered rises. The deformation recovery rate increases with increasing amounts of the hard segment, and reaches values of up to 99 % for the material synthesized from a poly(tetrahydrofuran) with  $M_n = 250$  and a hard-segment content of 75 wt %. Complete recovery of materials prepared from a switching segment with  $M_n = 650$  is only reached for a hard-segment content of 87 % and higher. A constant recovery rate of 95 % is reached after approximately 100 repetitions of the bending experiment. If the deformation recovery rate is plotted against the temperature, an increase in the switching temperature with increasing  $T_g$ , or increasing hard-segment content, can be found, as expected.

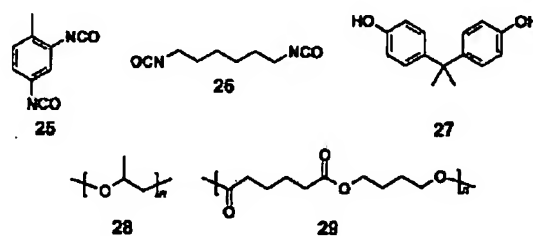
Materials obtained from low molecular weight poly(tetrahydrofurans) but with a high weight fraction of the hard-segment-forming phase show more or less complete deformation recovery. The block copolymers with high amounts of hard segments (between 67 and 95 wt %) show almost complete recovery, independent of the molecular weight of poly(tetrahydrofurans). The deformation recovery rate is higher as the molecular weight of the switching segment decreases. This effect is caused by an increased restriction of the shorter switching-segment chains to coil themselves. A large amount of hard-segment-determining blocks limits the twisting and coiling of the switching segment chains and thus considerably controls the shape-memory properties. In materials with high molecular weight poly(tetrahydrofuran) blocks, the hard-segment-determining blocks can not fulfill this task effectively. Here, the more intense twisting of the chains clearly results in lower recovery rates. This effect can only be compensated for by increasing the proportion of hard-segment-determining blocks.

Block copolymers containing a hard-segment-forming phase of MDI and 1,4-butanediol and a switching segment based on poly(ethylene adipate) (24) can be triggered by a glass transition temperature.<sup>[11]</sup> The glass transition temperature obtained with switching segment blocks with weight-average molecular weights of 300, 600, and 1000 at a constant hard segment content of 75 mol % decreases from 48 to -5 °C with increasing molecular weight of the poly(ethylene adipate)diols used. The  $T_g$  value of the switching-segment phase in a block copolymer prepared from poly(ethylene adipate)diol with a molecular weight  $M_w = 600$  increases from 13 to 35 °C as the hard-segment content increases (from 75 to 90 mol %). This effect is caused by an increased hindrance in the mobility of the switching-segment chains. Cyclic, thermomechanical tensile tests ( $\epsilon_m = 100\%$ ) of a material synthesized from a polymer with  $M_w = 600$  and a hard segment content of 88 mol % (69 wt %) show that the remaining strain after recovery  $\epsilon_p$  increases with the number of cycles. The strain recovery rate decreases from 85 % after the first cycle to 70 % after the fourth cycle. This behavior is a sign of increased

fatigue in the material as the number of cycles increases; this fatigue is caused by an increase in the slippage of the amorphous segments.

Since the 1980s Mitsubishi Heavy Industries have marketed shape-memory polymers that are triggered by means of a glass transition temperature. Hayashi and co-workers have described polyurethane systems with shape-memory properties that exhibit a glass transition temperature in the range between -30 and 30 °C and discussed their application as auto chokes or thermosensitive switching valves.<sup>[9, 58]</sup> An extension of these polyurethane systems was described in a patent in 1992.<sup>[59]</sup> Here, materials with glass transition temperatures in the range of -45 to 48 °C are described. This patent refers to the production of fabrics using threads made of polyurethane elastomers showing the shape-memory effect. These are supposed to enhance the crease resistance of the fabrics. Other applications discussed are moisture-permeable membranes in breathable fabrics whose permeability shows a sharp rise above the  $T_g$  value because of a higher segment mobility.

Table 2 presents a summary of the possible composition of the hard-segment- and the switching-segment-forming phases prepared at Mitsubishi. The hard-segment-determining blocks can be formed by toluene-2,4-diisocyanate (25, 2,4-TDI), MDI (18), carbodiimide-modified diisocyanates such as MDI and hexamethylene diisocyanate (26, HDI), and chain extenders such as ethylene glycol, bis(2-hydroxyethyl)hydroquinone, or a combination of 2,2'-bis(4-hydroxyphenyl)propane (27, bisphenol A) and ethylene oxide. The switching-



segment-determining blocks can be formed by polyethers, for example, PEO (13,  $M_n = 600$ ), poly(propylene oxide) (28,  $M_n = 400, 700, 1000$ ), poly(tetrahydrofuran) (17,  $M_n = 400, 650, 700, 850, 1000$ ), or a combination of bisphenol A and propylene oxide ( $M_n = 800$ ), or oligoesters, for example, poly(butylene adipate) (29,  $M_n = 600, 1000, 2000$ ).

The results of cyclic, thermomechanical tensile tests with maximum elongations  $\epsilon_m$  of 50 and 100 % for two materials differing in E modulus above their  $T_g$  values of 45 °C are reported: one material with polyester switching blocks and a relatively high E modulus and another material with polyether switching blocks with a low E modulus. In the course of the cyclic, thermomechanical tensile test, the test pieces were stretched at a temperature  $T_{high}$  of 65 °C to the maximum elongation  $\epsilon_m$  mentioned above. The samples were then cooled down to a temperature  $T_{low}$  of 25 °C and kept for five minutes at this temperature—the deformation was fixed by cooling below the system's glass transition temperature. Subsequently, the external stress was released, the sample

was heated to  $T_{\text{high}}$ , and the recovery caused by the thermally induced shape-memory effect was recorded. The next cycle was then started. The strain remaining after the materials recovery  $\epsilon_p$  increases with a growing number of cycles. The strain recovery rate already decreases during the first 4–5 cycles, which indicates an increasing fatigue of the material or a deterioration of the shape-memory properties. This behavior is interpreted in terms of an irreversible slipping of the chains within the amorphous segments, disentangling of mechanical entanglements, and a partial breakage of the crystalline hard segments especially after the first two cycles. The best strain recovery rates for an applied maximum elongation  $\epsilon_m$  of 50 and 100 % are observed for the polyether-based material (Table 10).

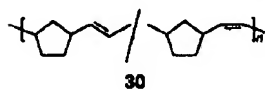
Table 10. Strain recovery rate after the first and fourth cycle. The values are calculated from Figures 6 and 9 in ref. [9].

Switching segment	$\epsilon_m$ [%]	$R_r(1)$ [%]	$R_r(4)$ [%]
polyester	50	80	70
polyester	100	85	80
polyether	50	85	75
polyether	100	90	85

#### 2.4.2. Other Thermoplastic Polymers

##### Polynorbornene

Norsorex is a linear, amorphous polynorbornene **30** developed by the companies CdF Chemie/Nippon Zeon in the late 1970s. The molecular weight of this polynorbornene is about  $3 \times 10^6$ .<sup>[8, 9]</sup> It is synthesized by a ring-opening metathesis



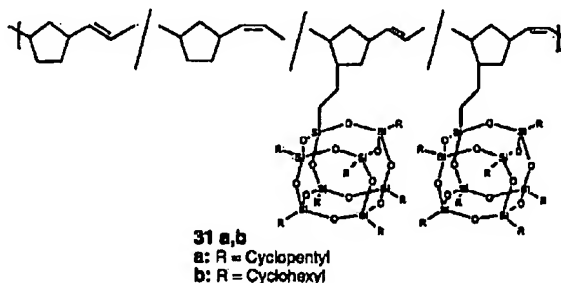
**30**

polymerization of norbornene using a tungsten–carbene complex as catalyst. The obtained polynorbornene contains 70 to 80 mol % of *trans*-linked norbornene units and has a glass transition temperature between 35 and 45 °C.<sup>[96, 97]</sup> The shape-memory effect of this strictly amorphous material is based on the formation of a physically cross-linked network as a result of entanglements of the high molecular weight linear chains, and on the transition from the glassy state to the rubber-elastic state (see Section 2.1.1).<sup>[98]</sup> The material softens abruptly above the glass transition temperature  $T_g$ . If the chains are stretched quickly in this state and the material is rapidly cooled down again below the glass transition temperature the polynorbornene chains can neither slip over each other rapidly enough nor disentangle. It is possible to freeze the induced elastic stress within the material by rapid cooling. Therefore, the sum of the time period for the stretching process  $\Delta t_{\text{stretch}}$  and the cooling process  $\Delta t_{\text{cool}}$  has to be much shorter than the time period it would take the stretched system to relax  $\Delta t_{\text{relaxation}}$  ( $\Delta t_{\text{stretch}} + \Delta t_{\text{cool}} \ll \Delta t_{\text{relaxation}}$ ). The recovery of the material's original shape can be observed by heating again to a temperature above  $T_g$ . This occurs because of the thermally induced shape-memory effect.<sup>[99]</sup>

The norsorex described is not inevitably purely amorphous. Sakurai and Takahashi have reported a high molecular weight

polynorbornene with a high proportion of *trans*-linked norbornene units showing a tendency towards strain-induced crystallization.<sup>[96, 97]</sup> A material that has been stretched four times at 90 °C and has been cooled down rapidly to 0 °C, then exhibits a melting point of 85 °C. Wide-angle X-ray scattering (WAXS) analysis shows X-ray reflections that can be attributed to *cis* and *trans* crystallites. The intensity of these reflections correlates with the content of *cis* and *trans* crystallites. On the basis of this observation, the possibility must not be excluded that crystallites acting as physical netpoints contribute to the shape-memory effect.

Organic–inorganic hybrid polymers consisting of polynorbornene units that are partially substituted by polyhedral, oligomeric silsesquioxanes (POSS, that is, polycyclic silicon–oxygen compounds of the general formula  $\text{Si}_n\text{H}_m\text{O}_n$ ) also form an amorphous polynorbornene material.<sup>[99]</sup> The hydrogen atoms of the POSS units are either substituted by cyclohexyl or cyclopentyl substituents (**31a, b**). A POSS-modified polynorbornene is obtained with a content of 60 to



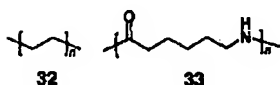
73 mol % *cis*-linked norbornene units by a ring-opening metathesis polymerization of hybrid-POSS-norbornene monomers and norbornene using a molybdenum catalyst. Up to 8.4 mol % or 50 wt % of the POSS-modified norbornene can be incorporated into the polynorbornene material by using this copolymerization process. The weight-average molecular weights obtained are in the range between 75 000 and 740 000. The glass transition temperature increases from 52 °C for pure polynorbornene (60 mol % *cis* content) to 81 °C in the case of a polynorbornene with a content of 50 wt % of a POSS norbornene with cyclohexyl substituents.

The increase in the glass transition temperature of the polynorbornene by incorporation of the POSS modified comonomers results in an improved heat and oxidation resistance. It is the C–C double bond in each repeating unit that makes pure polynorbornene sensitive towards oxidation. It should be possible to obtain better shape-memory properties by increasing the glass transition temperature to additionally slow down the relaxation of the polynorbornyl chains after stretching above  $T_g$ . WAXS investigations show that the material with cyclohexyl substituents is amorphous, like pure polynorbornene, whereas the POSS groups aggregate within the material containing cyclopentyl substituents and show phase separation to a certain extent. This arrangement of the side groups provides an additional physical cross-link and hence a stabilization of the material above  $T_g$ .

Clearly, better shape-memory properties can be observed relative to pure polynorbornene or the polynorbornene materials with POSS co-monomers bearing cyclohexyl substituents. If a maximum elongation  $\epsilon_m$  of 300% is applied, both the pure polynorbornene and the POSS-modified polynorbornene with cyclopentyl substituents show a strain recovery rate of approximately 75% upon heating to a temperature above  $T_g$ . If the recovery experiment is performed under a stress of 0.8 MPa for the polynorbornene homopolymer, because of the increased softening at temperatures above  $T_g$  after reaching the maximum recovery of 75% at a temperature of 70°C, again a stretching to over 200% at a temperature of 90°C can be observed. However, the polynorbornene with a content of 50 wt % POSS-modified norbornene with cyclopentyl substituents retains its shape even at high temperatures (up to 130°C) because of the stabilization described.

#### 2.4.2.2. Polyethylene/Nylon-6-Graft Copolymer

Polyethylene (32, PE) grafted with nylon-6 (33) that has been produced in a reactive blending process of PE with nylon-6 by adding maleic anhydride and dicumyl peroxide shows shape-memory properties.<sup>[100]</sup> The nylon-6 content of



these materials is between 5 and 20 wt %. Nylon-6, which has a high melting temperature of around 220°C, comprises the hard-segment-forming domains (domain size below 0.3  $\mu\text{m}$ ) in a matrix of semicrystalline PE. These domains form stable physical netpoints. The switching temperature for the thermally induced shape-memory effect is given by the melting point of the PE crystallites of 120°C. The polyethylene crystallites act as molecular switches. Strain fixity rates of around 99% and strain recovery rates between 95 and 97% have been determined for these materials for an elongation  $\epsilon_m$  of 100% (see Table 11). For nylon-6 contents between 5 and 20 wt %, no definite influence of the nylon content on the shape-memory properties can be found. The highest recovery rate has been determined to be at 120°C  $\pm$  2 K, which is in the range of the melting temperature of the PE crystallites. The shape-memory properties of PE cross-linked by treatment with ionizing radiation are given in Table 11 for comparison.

Table 11. Dependence of the strain recovery rate ( $R_r$ ) and strain fixity rate ( $R_f$ ) on nylon-6 content. The values are taken from Table 3 in ref. [100].

Material	$R_r$ [%]	$R_f$ [%]
LDPE cross-linked with ionizing radiation	94.4	96
PE with 5 wt % nylon-6	95.0	99.8
PE with 10 wt % nylon-6	94.9–96.9	99.0–99.5
PE with 15 wt % nylon-6	96.0	98.9
PE with 20 wt % nylon-6	96.6	98.6

## 2.5. Chemically Cross-Linked Shape-Memory Polymers

There are two strategies for the synthesis of polymer networks. Firstly, the polymer network can be synthesized by polymerization, polycondensation, or polyaddition of difunctional monomers and macromonomers by the addition of tri- or higher functional cross-linkers. Figure 7a shows the synthesis of covalently bound networks by treating methacrylate

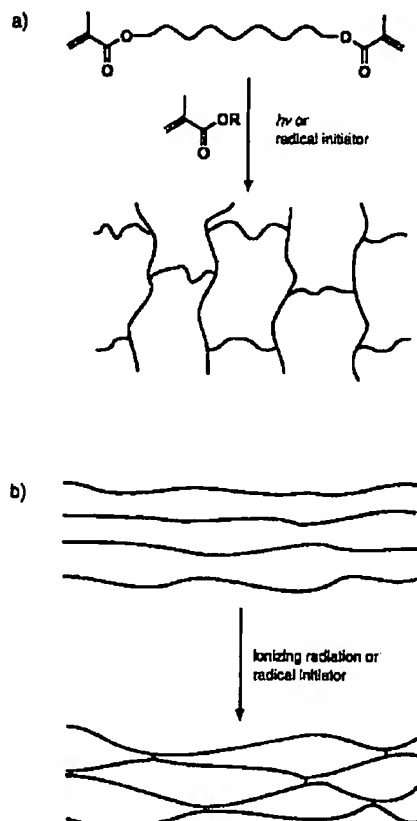


Figure 7. Synthesis strategies for polymer networks a) by polymerization or b) by cross-linking of linear polymers.

monomers with an oligomeric dimethacrylate as a cross-linker. The chemical, thermal, and mechanical properties of the network can be adjusted by the choice of monomers, their functionality, and the cross-linker content. The second strategy to obtain polymer networks is the subsequent cross-linking of linear or branched polymers (Figure 7b). In all the methods aimed at subsequent cross-linking of linear polymers the structure of the obtained network is strongly dependent on the reaction conditions and curing times, especially the cross-link density. The cross-linking of linear polymers can take place by a radical mechanism involving ionizing radiation or by the elimination of low molecular weight compounds to generate unsaturated carbon bonds. These have the capability to form chemical cross-links. The addition of radical initiators to linear polymers makes it possible to convert polymer chains into radicals that are able to recombine intermolecularly.

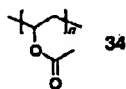
In the following section examples of the synthesis of shape-memory polymer networks for both synthetic strategies are presented. Polymers cross-linked by means of ionizing radiation have particular economic significance.

### 2.5.1. Network Synthesis by Subsequent Cross-Linking of Linear Polymers

#### 2.5.1.1. Polymers Cross-Linked by Means of Ionizing Radiation

Charlesby was the first to describe the "memory effect" of polyethylene treated with ionizing radiation ( $\gamma$  rays or neutrons).<sup>[2]</sup> A chemically cross-linked network is formed by application of low doses of irradiation. Polyethylene chains are orientated upon application of mechanical stress above the melting temperature of the polyethylene crystallites, which can be in the range between 60 and 134°C. Polyethylene crystals are formed by cooling below its crystallization temperature, and these can fix the temporary shape by acting as physical netpoints. Heating the material above the melting temperature of the crystalline domains results in the material returning to its permanent shape, which was fixed during the irradiation process.<sup>[2, 101]</sup>

This technology has reached high economic significance in the field of heat-shrinkable products. Materials that are most often used for the production of heat-shrinkable polymers are HDPE, LDPE, and copolymers of PE and poly(vinyl acetate) (34).<sup>[3, 5, 6]</sup> After shaping, for example, by extrusion or compression molding, the polymer is covalently cross-linked by means of ionizing radiation, for example, by highly accelerated electrons having energies of 0.5 to 3 MeV. The energy and dose of the radiation have to be adjusted to the geometry of the sample to reach a sufficiently high degree of cross-linking and hence



sufficient fixation of the permanent shape. The radiation dose should reach values between 20 and 30 Mrad (200–300 kGy). Subsequently, the preformed parts are heated above the melting temperature of the crystallites. At this temperature the material has rubber-elastic or viscoelastic properties. The samples formed in this state and then cooled down keep their temporary shape in the cooled state. The technical term for this process is "expansion". Commercial products have expansion ratios of up to 6:1. Depending on the intended application, heat-shrinkable products made of cross-linked, semicrystalline polymers are delivered either as semifinished products, for example, as heat-shrinkable tubing, or as the final products in the expanded state. These are connected to a substrate by a heat treatment. Areas of applications are, among others, the packing industry, electronic, civil, and process engineering.

The influence of the degree of cross-linking of  $\gamma$ -cross-linked PE on the gel content and heat-shrink properties was described for LDPE and HDPE.<sup>[102]</sup> The gel content increases with the applied radiation dose (0–160 kGy). For both materials, the gel point is exceeded by application of radiation doses between 11 and 22 kGy. A higher gel content is reached at the same dose for HDPE. The gel content reaches values of

around 60% for radiation doses of 160 kGy. At a dose of 100 kGy, the heat shrinkage is between 94 and 100% ( $T = 130^\circ\text{C}$ ) for LDPE and 100% ( $T = 150^\circ\text{C}$ ) for HDPE. Both the applied radiation dose and the shrink temperature chosen have a decisive influence on the heat shrinkage is reached: it increases with increasing radiation dose and temperature.

#### 2.5.1.2. Networks Synthesized by Subsequent Chemical Cross-Linking

Heating poly(vinyl chloride) (35, PVC) under a vacuum results in the elimination of hydrogen chloride in a thermal dehydrochlorination reaction. The material can be subsequently cross-linked in an HCl atmosphere. The polymer network obtained shows a shape-memory effect. Skákalová et al. have dehydrochlorinated a non-cross-linked PVC with a number-average molecular weight of about 50000 and subsequently cross-linked it.<sup>[103]</sup> The degree of dehydrochlorination varied between 0.6 and 86%. At the beginning of the dehydrochlorination reaction a strongly cross-linked structure is formed. Afterwards, an increasing degradation of the chains takes place that is accompanied by a loss in the thermal and mechanical stability of the material.

The shape-memory effect of the material was recorded on observing the recovery of a sample, which had been compressed before, with an original volume  $V_0$  upon heating above the glass transition temperature of about  $83^\circ\text{C}$  by means of dilatometry [Eq. (9)]. The highest relative increase

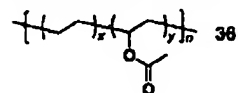
$$\varepsilon(T) = \frac{\Delta V(T)}{V_0} \quad (9)$$

in volume  $\Delta V(T)$  with values  $\varepsilon(T)$  of 2.0 is reached by samples with a degree of dehydrochlorination of 12.9 and 22.5% at a temperature of  $100^\circ\text{C}$ . The very weakly dehydrochlorinated sample (degree of dehydrochlorination of 0.6%) shows almost no recovery. Samples with a degree of dehydrochlorination of 2.6 and 54.4% exhibit an increase in their relative volume  $\varepsilon(T)$  of 1.0.

#### Polyethylene–Poly(vinyl acetate) Copolymers

Cross-linked poly[ethylene-co-(vinyl acetate)] is produced by treating the radical initiator dicumyl peroxide with linear poly[ethylene-co-(vinyl acetate)] (36) in a thermally induced cross-linking process.<sup>[104]</sup> Materials with different degrees of cross-linking are obtained depending on the initiator concentration, the cross-linking temperature, and the curing time.

The gel content of the obtained cross-linked materials can be used as an estimate of the degree of cross-linking. The co-monomer vinyl acetate, which is randomly incorporated into poly(ethylene-co-vinyl acetate) by copolymerization, causes a decrease in the melting temperature of polyethylene crystallites relative to the PE homopolymer. A copolymer having a vinyl acetate content of 28 wt% shows a melting temperature of  $70^\circ\text{C} \pm 1.5\text{ K}$  for the polyethylene crystallites. The cross-linking does not significantly influence the melting temperature. The values obtained



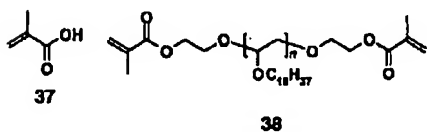
for strain fixity and strain recovery rates at a maximum elongation  $\epsilon_m$  of 100% for materials which have been cross-linked at 170°C are shown in Table 12. To determine these properties, polymer samples were heated up to 80°C, stretched to  $\epsilon_m = 100\%$ , and cooled down quickly to fix the deformation. A strain recovery is observed upon heating the sample up to 90°C. The strongest recovery effect is found at temperatures just above 60°C, which is close to the melting point. The strain recovery rate for polymer networks having gel contents lower than 30% already decreases strongly during the first four thermocycles. In contrast, the strain recovery rates of polymer networks which are cross-linked more strongly, with gel contents higher than 30%, stay constant or increase during the first four cycles.

Table 12. Dependence of the strain recovery rate ( $R_r$ ) and strain fixity rate ( $R_f$ ) on gel content of poly[ethylene-co-(vinyl acetate)] (EVA) as an estimate for the degree of cross-linking. The values are taken from Table 3 in ref. [104].

Sample (gel content)	$R_r$ [%]	$R_f$ [%]
EVA non-cross-linked	34.8	99.0
EVA (3.2%)	40.0	98.5
EVA (5.5%)	50.0	97.5
EVA (10.5%)	68.3	97.7
EVA (33.5%)	94.2	96.1
EVA (41.5%)	98.3	95.0

### 2.5.2. Synthesis of Shape-Memory Networks by Copolymerization of Monofunctional Monomers with Low-Molecular Weight or Oligomeric Cross-Linkers

Covalently cross-linked copolymers made from stearyl acrylate, methacrylate (37), and *N,N'*-methylenebisacrylamide as a cross-linker exhibit a shape-memory effect. The thermal transition triggering the shape-memory effect is the melting point of the crystalline domains formed by the stearyl side chains. The content of stearyl acrylate varies between 25 and 100 mol %. The melting/switching temperatures  $T_{\text{trans}}$  for the shape-memory effect are found between 35°C for a stearyl acrylate content of 25 mol % and 50°C for pure stearyl acrylate cross-linked by *N,N'*-methylenebisacrylamide. The temporary shape is programmed by stretching the sample at 60°C and then cooling. The permanent shape will be recovered if the polymer sample is heated up above the switching temperature.<sup>[105]</sup>



Multiphase copolymer networks are obtained by radical copolymerization of poly(octadecyl vinyl ether)diacrylates (38) or -dimethacrylates with butyl acrylate. The octadecyl side chains can crystallize because of the phase separation. The poly(octadecyl vinyl ether)diacrylates used in the synthesis have number-average molecular weights of around 5000. The poly(octadecyl vinyl ether) contents are between 20

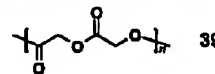
and 100 wt %. The melting point of the crystalline domains of 41 to 42°C is independent of the octadecyl vinyl ether content, which supports the assumption of almost complete phase separation. A strain fixity rate of 83% is reached upon stretching a polymer sample to  $\epsilon_m = 100\%$  at 60°C and subsequent cooling. A further heating up to 60°C initiates the shape-memory effect. The materials recovery is described as being complete. However, the strain recovery rate was not quantified more precisely with respect to the composition of the material.<sup>[106, 107]</sup>

## 2.6. Biodegradable Shape-Memory Polymer Systems

A very promising field in which shape-memory polymers can be the enabling technology for future applications, is the area of biomedicine.<sup>[1, 108, 109]</sup> Synthetic, degradable implant materials have led to dramatic progress in a variety of medical treatments. The highly innovative potential of degradable biomaterials is opposed by the time-consuming and cost-intensive procedure for obtaining approval for use in medical devices. In the next section, a short overview about well-established materials used for implants is followed by the introduction of degradable implant materials which exhibit a thermally induced shape-memory effect.

### 2.6.1. Degradable Implant Materials

Significant progress was made in surgical procedures at the beginning of the 1970s by the introduction of resorbable, synthetic implant materials as suture materials.<sup>[110, 111]</sup> These materials are polyhydroxycarboxylic acids, such as polyglycolide 39, or the copolyesters of L-lactic acid and glycolic acid. These aliphatic polyesters are still being used successfully today and have become a well established standard. Only a few other degradable polymers have been commercialized since that time. This fact is caused by the time-consuming and cost-intensive approval procedure for medical devices. An example of a group of materials which were developed in the 1980s are the polyanhydrides.<sup>[112]</sup> Based on a polyanhydride matrix, the implantable drug-delivery systems gliadel (treatment of brain tumors *glioblastoma multiforme*) and septicin (combat of chronic bone infections) have been developed. Polyanhydrides show surface erosion, while polyhydroxycarboxylic acids are degraded in the bulk.



The number of potential applications for degradable implant materials is growing constantly. On the one hand, the growing confidence of clinicians in the concept of degradable implants on the basis of the positive experience gained upon application of established materials have led to this trend. On the other hand, novel therapeutic concepts have been developed using the advantages of degradable biomaterials, for example, tissue reconstruction based on porous scaffolds, which can be cultivated with cells (tissue engineering).<sup>[113, 114]</sup>

The requirements for an implant material are determined by the specific application. The key properties of degradable biomaterials are their mechanical properties, their degrada-

tion rate, and degradation behavior, as well as biocompatibility and functionality. Each application requires a specific combination of these properties. With the growing number of potential applications, the number of materials needed that show different combinations of these properties is also increasing. However, the properties of the established biomaterials can only be varied in a limited range. Therefore, a new generation of degradable implant materials is needed.

The shape-memory polymers presented in the following section are considered to be promising candidates for the next generation of degradable implant materials. This concept is especially promising for these materials because it is a polymer system, that is, a group of polymers in which different macroscopic properties of the polymer can be varied virtually independently from each other in a wide range by only small changes in the chemical structure.

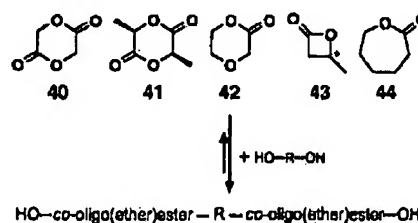
### 2.6.2. Polymer Systems with Shape-Memory Properties

Stimuli-sensitive implant materials have a high potential for applications in minimally invasive surgery. Degradable implants could be inserted into the human body in a compressed (temporary) shape through a small incision. When they are placed at the correct position, they obtain their application-relevant shape after warming up to body temperature. After a defined time period, the implant is degraded and becomes resorbed. In this case a follow-on surgery to remove the implant is not necessary.

Metallic shape-memory alloys such as nitinol are already used for biomedical applications as cardiovascular stents, guide wires, as well as orthodontic wires.<sup>[31]</sup> However, the mechanical properties of these alloys can only be varied in a limited range. The deformation between temporary and permanent shape is limited to 8% at best. Furthermore, the programming of these materials is time-consuming and demands temperatures of several hundred degree Celsius.<sup>[22c]</sup>

Designing degradable shape-memory polymers includes selecting suitable netpoints, which determine the permanent shape, and net chains, which act as switching segments. Furthermore, appropriate synthetic strategies have to be developed. The risk of possible toxic effects of polymers can already be minimized by selecting monomers whose homo- or copolymers have been proven to be biocompatible.

Appropriate switching segments for degradable shape-memory polymers can be found by considering the thermal properties of well-established degradable implant materials. The respective macrodiols, which can be used for the synthesis of shape-memory polymers, can be produced by means of ring-opening polymerization of lactones and cyclic diesters, such as 40–44, with a low molecular weight diol (Scheme 2). The sequence structure of the copolyesters can be influenced by polymerizing with or without catalyst. The molecular weight  $M_n$  could be adjusted between 500 and 10000 by the stoichiometric ratio of the starting materials.<sup>[115]</sup> For biomedical applications, a thermal transition of the switching segments in the temperature range between room and body temperature is of special interest. Two possible candidates were identified for use in this temperature range: poly( $\epsilon$ -caprolactone)diols, which exhibit a melting temperature  $T_m$



Scheme 2. Synthesis macrodiols from cyclic diesters and lactones.

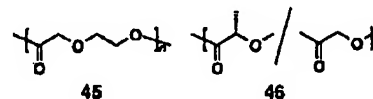
in the range of 46 and 64°C (see Table 3), as well as amorphous copolyesters of diglycolide 40 and dilactide, which have a glass transition temperature  $T_g$  in the range between 35 and 50°C.<sup>[110]</sup> However, one has to be aware that the decrease in glass transition temperature of macrodiols with decreasing chain length is attributed to the amount of freely moving chain ends. If the end groups of these telechelics are bonded covalently into a polymer, the decrease in the  $T_g$  value can no longer be observed.

The netpoints can either be of physical or chemical nature (see Section 2.1.2). In the following section one example for each case of a thermoplastic elastomer and a covalently cross-linked polymer network are described.

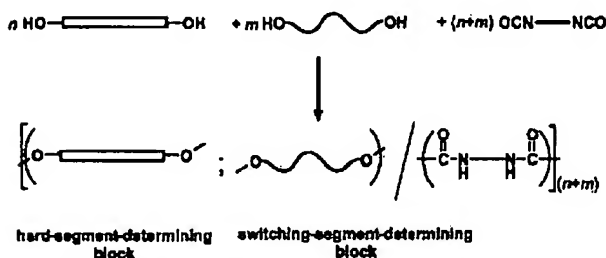
#### 2.6.2.1. Biodegradable Thermoplastic Elastomers with Shape Memory

A series of biocompatible and simultaneously biodegradable multiblock copolymers with shape-memory properties could be synthesized for the first time based on the macrodiols shown in Scheme 2. The thermoplastic elastomers resulting from the synthesis are elastic at room temperature and exhibit high elongation at break  $\epsilon_R$  of 650 to 1100% with tensile moduli between 34 and 90 MPa.<sup>[116]</sup>

On the one hand, these polymers are linear multiblock copolymers that have a crystallizable hard segment ( $T_m$ ) of poly( $p$ -dioxanone) (45) and an amorphous switching segment (here, poly[( $L$ -lactide)- $co$ -glycolide] (46) with a glycolide content of 15 mol %) that exhibits a glass transition temperature  $T_g$ . On the other hand, multiblock copolymers have been synthesized whose switching-segment-determining blocks consist of a crystallizable poly( $\epsilon$ -caprolactone) segment.



The thermoplastic elastomers are synthesized by a co-condensation of two different macrodiols by means of a bifunctional coupling agent, for example, diisocyanate, diacid dichloride, or phosgene (Scheme 3). It is necessary to reach high molecular weights with values of  $M_n$  in the range of 100000 to obtain the desired mechanical properties. The molecular parameters that determine this polymer system are the molecular weight, the microstructure (sequence), and the co-monomer ratio of the macrodiols as well as the hard-



Scheme 3. Synthesis of multiblock copolymers by the coupling of different macrodiols.

segment content within the multiblock copolymer. The new copolyester urethanes are completely hydrolytically degradable, and the degradation rate can be varied over a wide range (Figure 8). In contrast to the degradation behavior of several polyhydroxycarboxylic acids, mass loss can be observed quite early in the case of the shape-memory polymers under investigation. It is found that they become almost linear with degradation time.

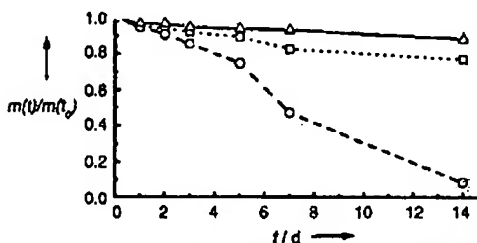


Figure 8. Hydrolytic degradation of different copolyester urethanes in aqueous buffer solution (pH = 7) at 70 °C. System A: Switching segment from poly(L-lactide-co-glycolide) with a content of 15 mol% glycolide with 30 wt % (○) and 40 wt % hard segment (◻); system B: switching segment from poly(ε-caprolactone) with 30 wt % hard segment (Δ).

### 2.6.2.2. Biodegradable Polymer Networks with Shape Memory

A polymer system with an AB polymer network structure has been developed based on oligo(ε-caprolactone)diol as the component that forms a crystallizable switching segment.<sup>[11]</sup> For that purpose, oligo(ε-caprolactone)diols have been functionalized with methacrylate end groups that can undergo a polymerization reaction. The co-monomer of choice was *n*-butyl acrylate because of the low  $T_g$  value of pure poly(*n*-butyl acrylate) (−55 °C) which is supposed to determine the soft segment of the resulting polymer network. The molecular weight of the used oligo(ε-caprolactone)dimethacrylate cross-linker and the co-monomer content of butyl acrylate represent the molecular parameters for controlling crystallinity as well as the switching temperature and mechanical properties. In contrast to the described process for the cross-linking of diacrylates by photopolymerization, in this case the cross-linking is performed without the addition of an initiator.<sup>[117]</sup> The number-average molecular weights of the oligo(ε-caprolactone)dimethacrylates used were 2000 and 10000. The cross-link density was varied by the addition of 11 to 90 wt % butyl acrylate in the case of the low molecular weight and by addition of 20 to 71 wt % butyl acrylate for the high

molecular weight oligo(ε-caprolactone)dimethacrylate. The cross-link density increases with decreasing content of butyl acrylate.

The butyl acrylate content influences the thermal properties of the AB network formed, especially for the oligo(ε-caprolactone)dimethacrylate with a molecular weight of 2000. Here, a melting point of  $T_m = 25$  °C can be observed only in the case of a very low content of butyl acrylate of 11 wt %. The corresponding homo-network of oligo(ε-caprolactone)dimethacrylate has a melting point of 32 °C. All the other networks of this series were found to be completely amorphous. For the networks of butyl acrylate and oligo(ε-caprolactone)dimethacrylate having a number-average molecular weight of 10000, the melting point decreases by up to 5 K to 46 °C with increasing butyl acrylate content.

The mechanical properties of both materials containing oligo(ε-caprolactone) segments with number-average molecular weights of 2000 or 10000 change significantly with increasing butyl acrylate content. The values of the elastic modulus, the tensile strength  $\sigma_m$ , and the tensile stress at break  $\sigma_R$  decrease by approximately an order of magnitude. The absolute values are one order of magnitude higher for the series with the oligo(ε-caprolactone) segments having number-average molecular weights of 10000. Strain fixity rates between 95 and 85 % as well as strain recovery rates from 98 to 93 % could be obtained in cyclic, thermomechanical tensile tests of the network containing the higher molecular weight oligo(ε-caprolactone) segments. All materials reached a constant strain recovery rate of 99 % after three thermocycles (Figure 9).

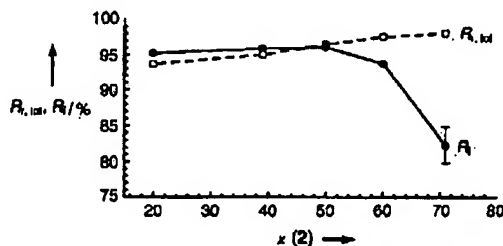


Figure 9. Shape recovery rate  $R_{rec}$  and shape fixity rate  $R_f$  as a function of butyl acrylate (2) content  $x$  (in wt %).

## 3. Summary and Outlook

Shape-memory polymers belong to the group of intelligent ("smart") polymers. They have the capability to change their shape on exposure to an external stimulus. This article has given an overview of the state of the art and the future potential of the shape-memory technology for polymers with a thermally induced one-way effect. The polymer switches from its actual, temporary shape to its memorized, permanent shape when it exceeds the switching temperature  $T_{trans}$ .

This shape-memory technology consists of two components: on the one hand the polymer architecture or morphology has to fulfill certain structural requirements, and on the other hand a special processing and programming technology is needed. Optimizing these two components includes the application of special characterization techniques. In partic-

ular cyclic, thermomechanical measurements are performed. These methods allow not only quantification of the shape-memory effect but also optimization of programming parameters ( $T_{low}$ ,  $T_{high}$ , heating rates,  $\epsilon_m$ , etc.). A detailed knowledge of the molecular mechanism of the shape-memory effect and of the corresponding structure/property relationships is necessary to understand the mutual dependencies of the different macroscopic effects. For example, the strain recovery rate  $R$ , not only depends on the kind of polymer but also on the strain  $\epsilon_m$  that describes the maximum deformation during the cyclic thermomechanical tensile test. Only a few data sets concerning the shape-memory properties of the polymers which are comparable to each other and systematically determined are described in the scientific literature. A complete data set comprises, in particular, a comprehensive characterization of the structure and composition of these polymers.

In the broadest sense, shape-memory polymers that show a thermally induced shape-memory effect are networks. The netpoints, which can either have chemical or physical nature, determine the permanent shape. The net chains show a thermal transition in the temperature range in which the shape-memory effect is supposed to be triggered. The temporary shape can be stabilized by the transition  $T_{trans}$  which is based on the switching segments. If a polymer contains several different blocks, mixed phases can be formed, to which a single mixed glass transition is attributed. The mixing behavior of the switching segment with other segments has to be considered during the design of the polymer. This is of particular importance if the shape-memory effect is triggered by a glass transition. If  $T_{trans}$  is a melting point the crystallization behavior of the switching segment can be influenced by modifying different programming parameters. These parameters include the cooling rate from  $T_{high}$  to  $T_{low}$ , the temperature  $T_{low}$  at which the polymer sample crystallizes, and the time period when the sample is held at  $T_{low}$ . Both the deformability from the permanent to the temporary shape and the recovery of the permanent shape can be attributed to entropy elasticity on the molecular scale (see Section 2.1.3).

Thermoplastic elastomers and covalent polymer networks differ not only in their properties but also in the corresponding processing and programming procedures. Certain limitations arise from the molecular structure of both types of materials. Block copolymers with shape-memory properties require a minimum weight fraction of hard-segment-determining blocks to ensure that the respective domains act as physical netpoints. Relaxation and reorganization processes, such as the sliding of chains in single domains, can complicate the programming of these materials. Covalently cross-linked shape-memory polymers can comprise a higher weight fraction of switching-segment-determining blocks compared to thermoplasts. Exceeding the switching transition may, in the case of a very high content of the switching segment, result in the occurrence of high stresses, which may, in an extreme example, cause damage to the sample.

As a result of their different profile qualities, both types of material, thermoplastic elastomers and covalently cross-linked polymer networks, are qualified for different applica-

tions. Therefore, both will have relevance for industrial applications in the future.

The handling of high molecular weight, amorphous polymers whose permanent shape is exclusively fixed by entanglements of the polymer chains within a certain time interval are challenging. For example, high precision for the programming as well as for the recovery process is necessary to avoid a flowing of the material. However, long-term storage of samples in their temporary shape is difficult because modification of the permanent shape by any type of relaxation processes may occur. Therefore, a broad range of applications for such materials is unlikely.

A group of implant materials with shape memory that have been developed for biomedical applications was described. These implant materials are not a single polymer with a specific composition but polymer systems which allow variation of different macroscopic properties within a wide range through only small changes in the chemical structure. For this reason a variety of different applications can be realized with tailor-made polymers of the same family. The polymers are mainly synthesized from a few monomers that are already used in the synthesis of established, degradable biomaterials. Both thermoplastic elastomers as well as covalently cross-linked polymer networks have been prepared and investigated. The synthesis of thermoplastic multiblock copolymers could successfully be scaled-up to the production of kilogram amounts in batch processes. Comprehensive *in vitro* investigations of their tissue compatibility are currently being performed. The first results are promising. In cooperation with physicians and biologists, concrete applications are being developed and tested in preclinical studies.

The thermally induced one-way shape-memory effect is not confined to polymers. It has also been described for other materials, especially for metallic alloys and gels. However, the mechanical properties of shape-memory alloys, such as nitinol, can only be varied over a limited range. Their strongest restriction is the maximum deformation of only 8% between their permanent and temporary shapes. Shape-memory polymers can be deformed to much higher degrees and elongation up to 1100% is possible. Their mechanical properties can be varied over a wide range, particularly in the case of polymer systems. Polymers are cheaper than metallic alloys. Their processing and programming is less complicated. The fast programming process of shape-memory polymers enables an implant to be individually adapted to the need of a patient in the operating theatre. In principle, shape-memory polymers differ from stimuli-sensitive hydrogels in their higher mechanical stability.

Potential applications for shape-memory polymers exist in almost every area of daily life: from self-repairing auto bodies to kitchen utensils, from switches to sensors, from intelligent packing to tools. Only a few of these applications have been implemented to date, since only a few shape-memory polymers have so far been investigated and even less are available on the market. The majority of these polymers have not been designed especially as shape-memory materials. Here, the material design is at its very beginning. Extensive innovations have to be anticipated because of the interesting economical prospects that have already been realized for the

shape-memory technology within a short time period. Besides other stimuli, such as light or electromagnetic fields, the two-way shape-memory effect will play a prominent role in future developments.

An example which illustrates the tremendous potential of the shape-memory technology are polymer systems with shape-memory properties which have specifically been developed for medical applications by applying modern methods of polymer chemistry and biomaterial science. These developments have resulted in available intelligent polymers with tailor-made properties. Degradable shape-memory polymers provide interesting advantages over metal implants. On the one hand a follow-on surgery to remove the implant can be avoided, and on the other hand such medical products can be introduced into the body by minimally invasive procedures through a small incision. In this way, patients benefit from a more gentle treatment and costs in health care can be reduced. In this sense, shape-memory implant materials have the potential to influence decisively the way medicinal products are designed in the future.

#### 4. Abbreviations

2,4-TDI	toluene-2,4-diisocyanate
BEBP	bis(2-hydroxyethoxy)biphenyl
BHBP	bis(2-hydroxyhexoxy)biphenyl
HDI	hexamethylene diisocyanate
HDPE	high density polyethylene
LDPE	low density polyethylene
MDI	methylenebis(phenylisocyanate)
NIPA	N-isopropylacrylamide
PAAM	polyacrylamide
PE	polyethylene
PEO	polyethylene oxide
PET	polyethylene terephthalate
PEU	polyester urethane
Poly(THF)	poly(tetrahydrofuran)
POSS	polyhedral, oligomeric silsesquioxane
PS	polystyrene
PVC	poly(vinyl chloride)
$R_i$	strain fixity rate
$R_r$	strain recovery rate
SC	switching segment content
$T_g$	glass transition temperature
$T_m$	melting temperature
$T_{trans}$	switching temperature
$\epsilon_m$	maximum strain in the cyclic thermomechanical test
$\sigma$	tensile stress

The authors are grateful to Dr. Karl Kratz and Dr. Werner Grasser for recording the series of pictures. Dr. Werner Grasser is acknowledged for his assistance in graphical presentation. For financial support we would like to thank the German Ministry for Education and Research (BMBF; BioFuture Award project no. 0311867), Fonds der Chemischen Industrie (FCI), and memoScience GmbH, Aachen.

Received: June 6, 2001 [A 475]

- [1] A. Lendlein, A. M. Schmidt, R. Langer, *Proc. Natl. Acad. Sci. USA* 2001, 98, 842–847.
- [2] A. Charlesby, *Atomic Radiation and Polymers*, Pergamon Press, Oxford, 1960, pp. 198–257.
- [3] S. Ota, *Radiat. Phys. Chem.* 1981, 18, 81–87.
- [4] W. Chen, K. Xing, L. Sun, *Radiat. Phys. Chem.* 1983, 22, 593–601.
- [5] G. Kleinbans, W. Starkl, K. Nuffer, *Kunststoffe* 1984, 74, 445–449.
- [6] G. Kleinbans, F. Heldenbain, *Kunststoffe* 1986, 76, 1069–1073.
- [7] S. Machi, *Radiat. Phys. Chem.* 1996, 47, 333–336.
- [8] K. Nakayama, *Int. Polym. Sci. Technol.* 1991, 18, T43–48.
- [9] H. Tobushi, S. Hayashi, S. Kojima, *JSM E Int. J. Ser. I* 1992, 35, 296–302.
- [10] S. Hayashi, S. Kondo, C. Giordano, Conference Proceedings of the Annual Technical Conference and Exhibition of Plastic Engineers, 1994, 1998–2001.
- [11] T. Takahashi, N. Hayashi, S. Hayashi, *J. Appl. Polym. Sci.* 1996, 60, 1061–1069.
- [12] H. Tobushi, S. Hayashi, A. Ikai, H. Hara, *J. Phys. IV* 1996, 6, 377–384.
- [13] B. K. Kim, S. Y. Lee, M. Xu, *Polymer* 1996, 37(26), 5781–5793.
- [14] F. Li, X. Zhang, J. Hou, M. Xu, X. Luo, D. Ma, B. K. Kim, *J. Appl. Polym. Sci.* 1997, 64, 1511–1516.
- [15] M. Wang, X. Luo, X. Zhang, D. Ma, *Polym. Adv. Technol.* 1997, 8, 136–139.
- [16] X. Luo, X. Zhang, M. Wang, D. Ma, M. Xu, F. Li, *J. Appl. Polym. Sci.* 1997, 64, 2433–2440.
- [17] B. K. Kim, S. Y. Lee, J. S. Lee, S. H. Baek, Y. J. Choi, J. O. Lee, M. Xu, *Polymer* 1998, 39, 2803–2808.
- [18] J. R. Lin, L. W. Chen, *J. Appl. Polym. Sci.* 1998, 69, 1563–1574.
- [19] J. R. Lin, L. W. Chen, *J. Appl. Polym. Sci.* 1998, 69, 1575–1586.
- [20] L. C. Chang, T. A. Read, *Trans. AIME* 1951, 189, 47.
- [21] W. J. Bühler, J. W. Gilfrich, R. C. Wiley, *J. Appl. Phys.* 1963, 34, 1475.
- [22] a) *Shape Memory Materials* (Eds.: K. Otsuka, C. M. Wayman), Cambridge University Press, Cambridge, 1998; b) K. Otsuka, C. M. Wayman in ref. [22a], pp. 1–48; c) T. Saburi in ref. [22a], pp. 49–96; d) T. Tadaki in ref. [22a], pp. 97–116; T. Maki in ref. [22a], pp. 117–132; e) Y. Suzuki in ref. [22a], pp. 133–148; f) J. van Humbeek, R. Stalmans ref. [22a], pp. 149–183; g) K. Uchino in ref. [22a], pp. 184–202; h) S. Miyazaki in ref. [22a], pp. 267–281.
- [23] Z. G. Wei, R. Sandström, S. Miyazaki, *J. Mater. Sci.* 1998, 33, 3743–3762.
- [24] Z. G. Wei, R. Sandström, S. Miyazaki, *J. Mater. Sci.* 1998, 33, 3763–3783.
- [25] J. Van Humbeek, *Mater. Sci. Eng.* 1999, A273–275, 134–148.
- [26] K. Otsuka, X. Ren, *Intermetallics* 1999, 7, 511–528.
- [27] M. Merkel in *Taschenbuch der Werkstoffe* (Eds.: M. Merkel, K.-H. Thomas), Fachbuchverlag Leipzig im Carl Hanser Verlag, Munich, 2000, pp. 358–368.
- [28] K. E. Wilkes, P. K. Liaw, *JOM* 2000, 10, 45–51.
- [29] D. Yang, *Mater. Des.* 2000, 21, 503–505.
- [30] D. Mantovani, *JOM* 2000, 10, 36–44.
- [31] P. Lipscomb, L. D. M. Nokes, *The Application of Shape Memory Alloys in Medicine*, Suffolk, MBP, 1996.
- [32] T. Hirai, H. Maruyama, T. Suzuki, S. Hayashi, *J. Appl. Polym. Sci.* 1992, 45, 1449–1451.
- [33] T. Hirai, H. Maruyama, T. Suzuki, S. Hayashi, *J. Appl. Polym. Sci.* 1992, 45, 1849–1855.
- [34] T. Aoyagi, F. Miyata, Y. J. Nagase, *J. Controlled Release* 1994, 32, 87–96.
- [35] Z. Hu, X. Zhang, Y. Li, *Science* 1995, 269, 525–526.
- [36] Y. Osada, A. Matsuda, *Nature* 1995, 376, 219.
- [37] M. Uchida, M. Kurosawa, Y. Osada, *Macromolecules* 1995, 28, 4583–4586.
- [38] X. Zhang, Y. Li, Z. Hu, C. L. Littler, *Chem. Phys.* 1995, 102, 551–555.
- [39] X. He, Y. Oishi, A. Takahara, T. Kajiyama, *Polym. J.* 1996, 28, 452–457.
- [40] Y. M. Lee, S. H. Kim, C. S. Cho, *J. Appl. Polym. Sci.* 1996, 62, 301–311.
- [41] Y. Li, Z. Hu, Y. Chen, *J. Appl. Polym. Sci.* 1997, 63, 1173–1178.
- [42] Y. Osada, J.-P. Gong, *Adv. Mater.* 1998, 10, 827–837.
- [43] P. Hron, J. Šlechtová, *Angew. Makromol. Chem.* 1999, 268, 29–35.
- [44] T. Miyata, N. Asami, T. Urugami, *Nature* 1999, 399, 766–769.

- [45] C. Alvarez-Lorenzo, O. Guney, T. Oya, S. Yasuzo, K. Masatoshi, E. Takashi, T. Yukikazu, I. Toru, K. Kenichi, T. Kazunori, W. Guoqiang, A. Y. Grosberg, S. Masamune, T. Tanaka, *Macromolecules* **2000**, *33*, 8693–8697.
- [46] P. J. Flory, *Principles of Polymer Chemistry*, Cornell University Press, Ithaca, 1969, pp. 432–494.
- [47] J. M. G. Cowie, *Chemie und Physik der synthetischen Polymeren*, Vieweg, Braunschweig, 1997, pp. 278–405; J. M. G. Cowie, *Polymers: Chemistry and Physics of Modern Materials 2nd ed.*, Chapman & Hall, London, 1991.
- [48] *Römp Lexikon Chemie*, Vol. 4, 10th ed. (Eds.: J. Falbe, M. Regitz), Thieme, Stuttgart, 1998, p. 2586.
- [49] G. Capaccio, I. M. Ward, *Colloid Polym. Sci.* **1982**, *260*, 46–55.
- [50] S. R. Chowdhury, I. K. Mishra, C. K. Das, *Polym. Degrad. Stab.* **2000**, *70*, 199–204; S. R. Chowdhury, C. K. Das, *J. Appl. Polym. Sci.* **2000**, *77*, 2088–2095.
- [51] T. L. Smith, *Polym. Eng. Sci.* **1977**, *17*, 129.
- [52] F. Li, J. Hou, W. Zhu, X. Zhang, M. Xu, X. Luo, D. Ma, B. K. Kim, *J. Appl. Polym. Sci.* **1996**, *62*, 631–638.
- [53] H. M. Jeong, J. B. Lee, S. Y. Lee, B. K. Kim, *J. Mater. Sci.* **2000**, *35*, 279–283.
- [54] H. M. Jeong, B. K. Kim, Y. J. Choi, *Polymer* **2000**, *41*, 1849–1855.
- [55] M. Wang, Z. Lide, *J. Polym. Sci. Part B* **1999**, *37*, 101–112.
- [56] K. Sakurai, Y. Shirakawa, T. Kashiwagi, T. Takahashi, *Polymer* **1994**, *35*, 4238–4239.
- [57] P. van Caeter, E. J. Goethals, V. Gancheva, R. Velichkova, *Polym. Bull.* **1997**, *39*, 589–596.
- [58] Y. Shirai, S. Hayashi, *Mitsubishi Tech. Bull.* **1988**, *184*, 1–6.
- [59] K. Kobayashi, S. Shumichi (Mitsubishi Heavy Industries), US-A 5128197, 1992 (see <http://www.uspto.gov/patft/>).
- [60] R. M. Briber, E. L. Thomas, *J. Macromol. Sci. Phys. B* **1983**, *22*, 509.
- [61] J. R. Lin, L. W. Chen, *J. Appl. Polym. Sci.* **1998**, *69*, 1575.
- [62] C. G. Seefried, J. V. Koleske, F. E. Critchfield, *J. Appl. Polym. Sci.* **1975**, *19*, 2493.
- [63] J. R. Lin, L. W. Chen, *J. Appl. Polym. Sci.* **1998**, *69*, 1575.
- [64] F. Li, J. Hou, W. Zhu, X. Zhang, M. Xu, X. Luo, D. Ma, B. K. Kim, *J. Appl. Polym. Sci.* **1996**, *62*, 631–638.
- [65] D. B. Johns, R. W. Lenz, A. Luecke in *Ring Opening Polymerization*, Vol. 1, Elsevier, New York, 1984, pp. 461–521.
- [66] C. G. Pitt in *Biodegradable Polymers as Drug Delivery Systems*, Marcel Dekker, New York, 1990, pp. 71–120.
- [67] F. Li, J. Hou, W. Zhu, X. Zhang, M. Xu, X. Luo, D. Ma, B. K. Kim, *J. Appl. Polym. Sci.* **1996**, *62*, 631–638.
- [68] J. R. Lin, L. W. Chen, *J. Appl. Polym. Sci.* **1998**, *69*, 1575–1586.
- [69] U. Gaur, B. Wunderlich, *J. Phys. Chem.* **1981**, *10*, 1023.
- [70] J. R. Lin, L. W. Chen, *J. Appl. Polym. Sci.* **1998**, *69*, 1575–1586.
- [71] Ref. [69].
- [72] B. M. Grieverson, *Polymer* **1960**, *1*, 499.
- [73] *Römp Lexikon Chemie*, Vol. 5, 10th ed. (Eds.: J. Falbe, M. Regitz), Thieme, Stuttgart, 1998, p. 3449.
- [74] S. Fakirov, E. W. Fisher, G. H. Schmidt, *Makromol. Chem.* **1975**, *176*, 2459.
- [75] O. B. Edgar, R. Hill, *J. Polym. Sci.* **1952**, *8*, 1.
- [76] D. W. Woods, *Nature* **1954**, *174*, 753.
- [77] Laboratory Chemicals 2001/2002, Fluka Chemie GmbH, pp. 1231–1234.
- [78] U. Gaur, B. Wunderlich, *J. Phys. Chem.* **1981**, *10*, 1010.
- [79] H. Suzuki, B. Wunderlich, *J. Polym. Sci. Polym. Phys. Ed.* **1985**, *23*, 1671.
- [80] *Römp Lexikon Chemie*, Vol. 5, 10th ed. (Eds.: J. Falbe, M. Regitz), Thieme, Stuttgart, 1998, p. 3506.
- [81] R. Dedeurwaerder, J. F. M. Oth, *J. Chem. Phys.* **1959**, *56*, 940.
- [82] T. O. Fox, P. J. Flory, *J. Appl. Phys.* **1950**, *21*, 581.
- [83] F. P. Reding, I. A. Faucher, R. D. Whitmann, *J. Polym. Sci.* **1962**, *57*, 483.
- [84] M. Berger, D. J. Buckley, *J. Polym. Sci. A* **1963**, *1*, 2945.
- [85] G. Nata, *Science* **1965**, *147*, 269.
- [86] W. S. Bahary, D. I. Sapper, J. H. Lane, *Rubber Chem. Technol.* **1967**, *40*, 1529.
- [87] *Encyclopedia of Polymer Science and Engineering*, Vol. 6, Wiley, New York, 1986, p. 410.
- [88] *Encyclopedia of Polymer Science and Engineering*, Vol. 6, Wiley, New York, 1986, p. 411.
- [89] U. Gaur, B. B. Wunderlich, B. Wunderlich, *J. Phys. Chem.* **1983**, *12*, 56.
- [90] *Römp Lexikon Chemie*, Vol. 5, 10th ed. (Eds.: J. Falbe, M. Regitz), Thieme, Stuttgart, 1998, p. 3415.
- [91] *Encyclopedia of Polymer Science and Engineering*, Vol. 11, Wiley, New York, 1986, p. 366.
- [92] *Encyclopedia of Polymer Science and Engineering*, Vol. 11, Wiley, New York, 1986, p. 349.
- [93] T. G. Basari, A. Levy, M. Litt, *J. Polym. Sci. B* **1967**, *5*, 871.
- [94] M. Wang, X. Luo, D. Ma, *Eur. Polym. J.* **1998**, *34*, 1–5.
- [95] K. Sakurai, H. Tanaka, N. Ogawa, T. Takahashi, *J. Macromol. Sci. Phys. B* **1997**, *36*, 703–716.
- [96] K. Sakurai, T. Takahashi, *J. Appl. Polym. Sci.* **1989**, *38*, 1191–1194.
- [97] K. Sakurai, T. Kashiwagi, T. Takahashi, *J. Appl. Polym. Sci.* **1993**, *47*, 937–940.
- [98] P. T. Mather, H. G. Jeon, T. S. Haddad, *Polym. Prepr. Am. Chem. Soc. Div. Polym. Chem.* **2000**, *41*, 528–529.
- [99] P. T. Mather, H. G. Jeon, A. Romo-Uribe, *Macromolecules* **1999**, *32*, 1194–1203.
- [100] F. Li, Y. Chen, W. Zhu, X. Zhang, M. Xu, *Polymer* **1998**, *39*, 6929–6934.
- [101] A. Charlesby, *Proc. R. Soc. London* **1952**, *215*, 187–214.
- [102] S. Kumar, M. V. Pandya, *J. Appl. Polym. Sci.* **1996**, *64*, 823–829.
- [103] V. Skákalová, V. Lukáč, M. Breza, *Macromol. Chem. Phys.* **1997**, *198*, 3161–3172.
- [104] F. Li, W. Zhu, X. Zhang, C. Zhao, M. Xu, *J. Appl. Polym. Sci.* **1999**, *71*, 1063–1070.
- [105] Y. Kagami, J. P. Gong, Y. Osada, *Macromol. Rapid Commun.* **1996**, *17*, 539–543.
- [106] E. J. Goethals, W. Reynjens, S. Liévens, *Macromol. Symp.* **1998**, *132*, 57–64.
- [107] W. G. Reynjens, F. E. Du Prez, E. J. Goethals, *Macromol. Rapid Commun.* **1999**, *20*, 251–255.
- [108] M. Brennan, *Chem. Eng. News* **2001**, *79*(6), 5.
- [109] S. Ashley, *Sci. Am.* **2001**, No. 5.
- [110] A. Lendlein, *Chem. Unserer Zeit* **1999**, *33*, 279–295.
- [111] S. W. Shalaby, R. A. Johnson in *Biomedical Polymers* (Ed.: S. W. Shalaby), Hanser, München, 1994.
- [112] C. T. Laurencin, I. F. M. Sobrasua, R. S. Langer in *Biomedical Applications of Synthetic Biodegradable Polymers* (Ed.: I. O. Hollinger), CRC Press, Boca Raton, 1995.
- [113] J. D. Bronzino, *The Biomedical Engineering Handbook*, CRC Press, Boca Raton, 1995.
- [114] F. H. Silver, C. Doillon, *Biocompatibility: Interactions of Biological and Implantable Materials*, VCH-Wiley, New York, 1989.
- [115] A. Lendlein, P. Neuenchwander, U. W. Suter, *Macromol. Chem. Phys.* **2000**, *201*, 1067–1076.
- [116] A. Lendlein, R. Langer, *Science*, in press; published online on 25 April, 2002 as 10.1126/science.1066102 (Science Express Reports).
- [117] A. Nathan, D. Bolikal, N. Vyavahave, S. Zalipsky, J. S. Kuhn, *Macromolecules* **1992**, *25*, 4476–4484.

## SHAPE MEMORY EFFECT OF PU IONOMERS WITH IONIC GROUPS ON HARD-SEGMENTS\*

Yong Zhu, Jin-lian Hu\*\*, Kwok-wing Yeung, Hao-jun Fan and Ye-qiu Liu

*Institute of Textiles and Clothing, Hong Kong Polytechnic University, Hung Hom, Hong Kong, China*

**Abstract** SMPU (shape memory polyurethane) non-ionomers and ionomers, synthesized with poly( $\epsilon$ -caprolactone) (PCL), 4, 4'-diphenylmethane diisocyanate (MDI), 1,4-butanediol (BDO), dimethylolpropionic acid (DMPA) were measured with cyclic tensile test and strain recovery test. The relations between the structure and shape memory effect of these two series were studied with respect to the ionic group content and the effect of neutralization. The resulting data indicate that, with the introduction of asymmetrical extender, the stress at 100% elongation is decreased for PU non-ionomer and ionomer series, especially lowered sharply for non-ionomer series; the fixation ratio of ionomer series is not affected obviously by the ionic group content; the total recovery ratio of ionomer series is decreased greatly. After sufficient relaxation time for samples stretched beforehand, the switching temperature is raised slightly, whereas the recovery ratio measured with strain recovery test method is lowered with increased DMPA content. The characterization with FT-IR, DSC, DMA elucidated that, the ordered hard domain of the two series is disrupted with the introduction of DMPA which causes more hard segments to dissolve in soft phase; ionic groups on hard segment enhance the cohesion between hard segments especially at high ionic group content and significantly facilitate the phase separation compared with the corresponding non-ionomer at moderate ionic group content.

**Keywords:** Polyurethane; Ionomers; Cyclic thermo-mechanical investigations; Shape memory effect; Cyclic tensile test; Strain recovery test.

### INTRODUCTION

Segmented polyurethane (PU) has been investigated as shape memory polymer for its two-phase structure, fixed points or frozen phase and reversible phase<sup>[1–6]</sup>. Some of them could well fix the temporary shape with the crystallization structure of soft segments after deformation. In such materials, the crystalline soft domains form the reversible phase, with their crystalline melting temperature being the shape recovery temperature ( $T_i$ ), and hard domains become the fixed points or frozen phase. Fixed points remain hard during the second shaping process which normally is done at a temperature higher than the shape recovery temperature. Reversible phase is subject to softening and hardening upon heating above  $T_i$  and cooling below  $T_i$ , respectively.

Recently, it was found that PU ionomer species with phase separation morphology also have shape memory effect and especially, in some cases, have some specific tendency in mechanical property and thermal property, such as higher recovery strain, lower residual strain, higher hardness, increased modulus and strength as compared with non-ionomers for the Coulombic forces between the ionic centers positioned within the hard domains<sup>[3,7]</sup>. Kim *et al.*<sup>[3]</sup> systematically studied the effect of various soft segments content and lengths on the shape memory effect with cyclic tensile test. Meanwhile, with comparison of the dynamic mechanical properties and crystallization properties between the PU ionomer and the corresponding non-ionomer, Kim pointed out that the effect of the ionomer on micro-phase separation is two-fold. But the study about this two-fold effect and this

\* This work was supported by Hong Kong ITF research project (No. ITS 098/02).

\*\* Corresponding author: Jin-lian Hu(胡金莲), E-mail: tchujl@inet.polyu.edu.hk

Received April 7, 2005; Revised June 3, 2005; Accepted June 6, 2005

effect on shape memory properties has not yet been done. Jeong *et al.*<sup>[7]</sup> preliminarily investigated the shape memory properties of shape memory polyurethane ionomer based on poly( $\epsilon$ -caprolactone) (PCL), 4,4'-diphenylmethane diisocyanate (MDI), 1,4-butanediol (BDO), dimethylolpropionic acid (DMPA), hexamethylene diisocyanate (HDI), hexamethylene diamine (HAD) with a range of DMPA content from 1.5% to 4.5% just through the cyclic tensile test.

As for the quantitative study of shape memory effect, the cyclic thermo-mechanical investigations, shown in Fig. 1, is one of the most effective ways, as reported previously<sup>[8,9]</sup>. Some of researchers prefer to weigh shape memory properties only with the cyclic tensile test<sup>[2-4]</sup>, in which the strain recovery ratio  $R_r(N)$ , the total strain recovery ratio  $R_{r, \text{tot}}$ , the strain fixity ratio  $R_f(N)$ , can be calculated in term of the related Eqs. (1)–(3). Others tried to study the shape memory recovery behavior with the strain recovery test as shown in Fig. 2<sup>[11,10-13]</sup>, in which the heating rate will be fixed and the recovery temperature, recovery rate  $R_f$ , which could be calculated by the reversible length divided by original length,  $\epsilon_2$ , after stretching, will be figured as shown in the graph (b) of Fig. 2.

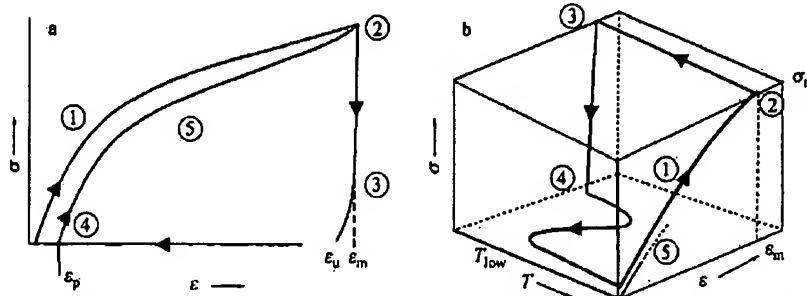


Fig. 1 Schematic representation of the results of the cyclic thermomechanical investigation for two different tests  
a)  $\epsilon$ - $\sigma$  diagram: ① Stretching to  $\epsilon_m$  at  $T_{\text{high}}$ ; ② Cooling to  $T_{\text{low}}$  while  $\epsilon_m$  is kept constant; ③ Clamp distance is driven back to original distance; ④ At  $\epsilon = 0\%$  heating up to  $T_{\text{high}}$ ; ⑤ Start of the second cycle  
b)  $\epsilon$ - $T$ - $\sigma$  diagram: ① Stretching to  $\epsilon_m$  at  $T_{\text{high}}$ ; ② Cooling down to  $T_{\text{low}}$  with cooling rate  $k_{\text{cool}} = dT/dt$  while  $\sigma_m$  is kept constant; ③ Clamp distance is reduced until the stress-free state  $\sigma = 0$  MPa is reached; ④ Heating up to  $T_{\text{high}}$  with a heating rate  $k_{\text{heat}} = dT/dt$  at  $\sigma = 0$  MPa; ⑤ Start of the second cycle

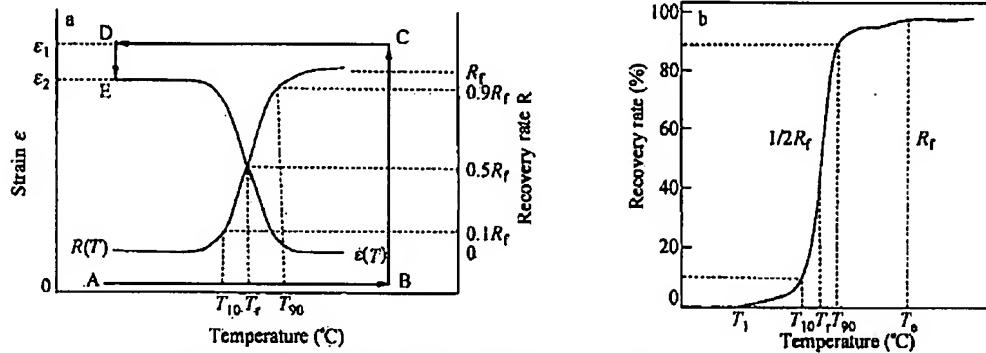


Fig. 2 Schematic representation of strain recovery test  
a) Diagram of preparation procedure of specimens for strain recovery measurements; b) Recovery curves,  $\epsilon$ - $T$

$$R_r(N) = \frac{\epsilon_m - \epsilon_p(N)}{\epsilon_m - \epsilon_p(N-1)} \quad (1)$$

$$R_{r, \text{tot}}(N) = \frac{\epsilon_m - \epsilon_p(N)}{\epsilon_m} \quad (2)$$

$$R(N) = \frac{\epsilon_s(N)}{\epsilon_m} \quad (3)$$

In this study, the cyclic tensile test and strain recovery test were combined to characterize the comprehensive shape memory property. To our best knowledge, the systematical study on shape memory polyurethane ionomer with cyclic thermo-mechanical investigations, including cyclic tensile test and strain recovery test, have not been reported yet. Moreover, Coulombic force between ionic groups on hard segments possibly can offer the cohesion between fixed points in shape memory polymer with the two-phase structure, which might comprise a part of the physical crosslink of fixed phase. Meanwhile, considering the advantages of such series of functional shape memory materials such as the low cost, simple processing, flexible transition temperature range, huge deformation between temporary and permanent shape, comparative low density, potential special properties such as antibacterial activity<sup>[14]</sup> and ionic conductivity<sup>[15]</sup>, it is necessary to deepen the study in this area so as to satisfy the requirement for the extensive application.

In the synthesis of PU samples, DMPA as a part of chain extender reagent is introduced into the hard segment of shape memory polyurethane. Through this way, the PU non-ionomer could be synthesized and the corresponding PU ionomer could be obtained by neutralizing all carboxyl groups of DMPA with the same amount of triethylamine (TEA). The DMPA content was gradually increased from 0 wt% to the maximum content, which is related to specific molecular structure, and other parameters about the molecule structure such as the soft segment content and soft segment length were fixed so as to investigate the effect of ionic group content on the properties of such series of materials. The thermal, crystallization, dynamic mechanical properties and shape memory effect were examined respectively.

## EXPERIMENTAL

### Material Preparation

The formula of the preparation of PU samples is shown in Table 1. PCL diols (Daicel Chemical Industries Ltd.) with molecular weight ( $M_n$ ) = 4000 were dried and degassed beforehand at 80°C under 0.1–0.2 kPa for 12 h for PU synthesis. Extra pure grade of MDI (Aldrich) and DMPA (Acros) were used to synthesize PU samples without further treatment. BDO (Acros) was dried by using molecular sieves in advance for several days. TEA (International Lab., USA) was used to neutralize the carboxyl groups of DMPA with the same mole.

Table 1. Formula of the polyurethane synthesis

Sample code	PCL (wt%)	DMPA (wt%)	Moles of PCL	Moles of DMPA	Moles of BDO	Moles of MDI	Moles of TEA
60-0	60	0	1	0	7.1	8.1	0
60-2I	60	2	1	1	6	8	1
60-5I	60	5	1	2.5	4.3	7.8	2.5
60-8I	60	8	1	4	2.6	7.6	4
60-10I	60	10	1	5	1.5	7.5	5
60-13I	60	13	1	6.3	0	7.3	6.3
60-2N	60	2	1	1	6	8	0
60-5N	60	5	1	2.5	4.3	7.8	0
60-8N	60	8	1	4	2.6	7.6	0
60-10N	60	10	1	5	1.5	7.5	0
60-13N	60	13	1	6.3	0	7.3	0

The reaction to prepare the pre-polymer with PCL and MDI was carried out at 80°C for 2 h in a 500 mL round-bottom, four-necked flask equipped with a mechanical stirrer, nitrogen inlet, thermo meter and condenser, followed by the chain extension with BDO and/or DMPA for the same period of time. Dimethylformamide (DMF) was used in PU synthesis as solvent and dehydrated with 4 Å molecular sieves for two days in advance. Thereafter, the neutralization reaction was followed at 40°C for 1 h by adding stoichiometric amount of TEA

agent. Before neutralization, some of PU solution was poured out from the flask for film casting of the corresponding PU non-ionomers. Films were prepared by casting the solution to Teflon pan, placed at 60°C for 24 h and further dried at 75°C under vacuum of 0.1–0.2 kPa for 24 h.

In this study, the soft segment content and soft segment length in PU ionomer and non-ionomer samples were controlled approximately to the same values, respectively so as to investigate the effect of ionic group content on the shape memory effect of PCL-4000 based SMPU. Two series of PU copolymers (non-ionomer and ionomer) were identified by the first number denoting the soft segment content, the second number representing the DMPA weight content and a letter showing the non-ionomers-"N" and ionomers-"I", such as 60-5I in which "60", "5" and "I" mean 60 wt% soft segment, 5 wt% DMPA content and ionomer charged with TEA respectively. The sample 60-0 contained no DMPA and just composed of MDI, BDO and PCL-4000 as comparison with the two series above.

#### *Differential Scanning Calorimetry*

Melting temperature of PU samples was determined by using Perkin-Elmer DSC-7 with nitrogen as purge gas. Indium and zinc standards were used for calibration. For the PU specimens from the same preparation process, firstly, samples were heated up to 240°C at a heating rate of 20 K/min and kept at 240°C for 3 min, subsequently, cooled to -50°C at a cooling rate of 20 K/min.

#### *Dynamic Mechanical Analysis (DMA)*

The sample film was prepared for DMA through film casting with a thickness of 0.5 mm, a width of 5 mm, and a length of 25 mm. Dynamic mechanical properties of the sample were determined by using a Perkin-Elmer DMA at 2 Hz, at a heating rate of 2 K/min from -100°C to 150°C.

#### *Attenuated Total Reflection-FT-IR*

Attenuated Fourier Infrared Spectra were determined with 0.5 mm thickness specimen film by using a Perkin-Elmer (2 000 FT-IR) spectrometer in the region of 700–4000  $\text{cm}^{-1}$  at room temperature. Each sample was scanned 30 times at a resolution of 2  $\text{cm}^{-1}$  and the scan signals were averaged. The region of carbonyl stretching vibration at 1700–1730  $\text{cm}^{-1}$  was used to detect changes of the extent of micro phase separation between PU non-ionomer and the corresponding PU ionomer studied. All IR spectra have been normalized by using the height of the 1412  $\text{cm}^{-1}$  peak, assigned to the C—C stretching mode of the aromatic ring<sup>[16]</sup>.

#### *Cyclic Tensile Test*

Cyclic tensile test was done by using an Instron 4466 apparatus with a temperature-controlled chamber, and a personal computer was used to control and record all data. First, the sample film with 5 mm width, 20 mm length and 0.5 mm thickness was heated to  $T_{\text{high}}$ , 60°C within 600 s. Then the sample was stretched to  $\epsilon_m$ , 100% elongation at  $T_{\text{high}}$ , 60°C with 10 mm/min stretching rate. After that, cool air will be introduced to the chamber for cooling sample film with constant strain,  $\epsilon_m$ , 100% elongation, to  $T_{\text{low}}$ , 20°C, within 900 s. Thereafter, the strain was released from  $\epsilon_m$  to 0 and the recurrent heating for 600 s began. That is one cycle among all cyclic tensile test and the cycle for each sample will be repeated four or five times for assessing the shape memory effect.

#### *Strain Recovery Test*

A microscopy (Leitz Wetzlar) with a hot stage (Mettler Toledo FP90 Central Processor & FP82 Hot Stage) and a camera (Pixera PVC 100C) were used to observe and record the strain recovery effect of sample film stretched in the cyclic thermal-mechanical investigation after one cycle. The heating rate of the recovery measurement was 2 K/min and the temperature range in heating process is from 25°C to 90°C.

## RESULTS AND DISCUSSION

#### *Effect of Ionic Groups on Crystallizability of SMPU Ionomer*

The thermograms of all the SMPU non-ionomers and the corresponding ionomes studied showed the endothermic melting peak of soft segment when heated as shown in Fig. 3. The data about thermal properties are

shown in Table 2. When the DMPA content is low enough such as 60-5I, the endothermic melting peak of hard segment of PU ionomer at around 162°C could be observed obviously. However, the corresponding PU non-ionomer 60-5N does not show the distinct melting peak of hard segment. The melting of hard segment crystals in all PU non-ionomer and the PU ionomer with the DMPA content higher than 5% could not be observed in DSC investigation. It could be due to the increased DMPA content on hard segment disrupts the ordered structure of hard domain. In comparison with the PU sample without DMPA such as 60-0, the melting point and enthalpy of melting of soft segment of PU non-ionomer and ionomer were increased. Just like the experimental result reported by Ahn and Kim *et al.*<sup>[7]</sup>, that with the increase of DMPA content, the enthalpy of soft segment of the two series generally increased. Especially for PU ionomers, this trend is more significant, and the increase of the melting enthalpy is higher than that of the corresponding PU non-ionomers, illustrating, in PU ionomers, there is higher crystallinity of soft segment compared with the PU non-ionomers.

Table 2. Thermal properties of PU non-ionomers and ionomers

Sample No.	Heating at 20 K/min				Cooling at 20 K/min			
	$T_{ms}$ (°C)	$\Delta H_{ms}$ (J/g)	$T_{mh}$ (°C)	$\Delta H_{mh}$ (J/g)	$T_{cs}$ (°C)	$\Delta H_{cs}$ (J/g)	$T_{ch}$ (°C)	$\Delta H_{ch}$ (J/g)
60-0	52	19.86	195.67	14.12	-5.1	12.29	161.9	8.85
60-5N	56.3	23.4	—	—	—	—	—	—
60-8N	56	27.7	—	—	—	—	—	—
60-10N	54.3	33.7	—	—	—	—	—	—
60-13N	56	31.9	—	—	—	—	—	—
60-5I	58	26.88	162.67	7.23	—	—	—	—
60-8I	57.3	35.64	—	—	—	—	—	—
60-10I	57.7	37.3	—	—	3.93	24.77	—	—
60-13I	56	38.16	—	—	3.93	32.43	—	—

$T_{ms}$ : melting temperature of soft-segment;  $\Delta H_{ms}$ : enthalpy of melting soft-segment;

$T_{mh}$ : melting temperature of hard-segment;  $\Delta H_{mh}$ : enthalpy of melting hard-segment;

$T_{cs}$ : temperature of soft-segment crystallization;  $\Delta H_{cs}$ : heat of soft-segment crystallization;

$T_{ch}$ : temperature of hard-segment crystallization;  $\Delta H_{ch}$ : heat of hard-segment crystallization

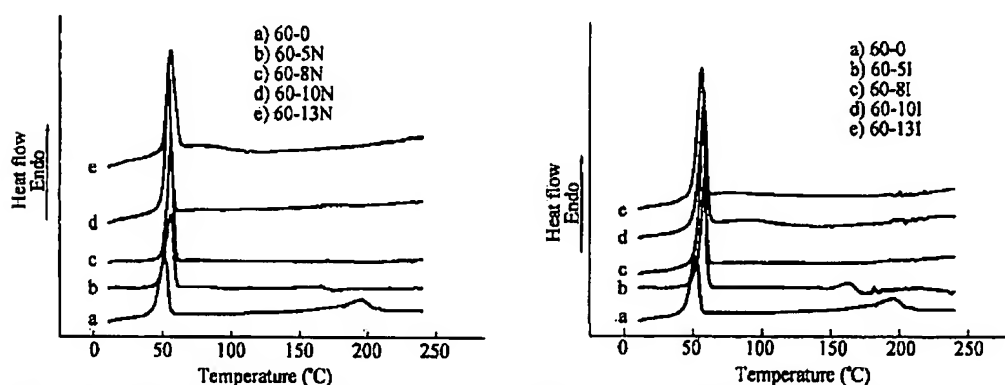


Fig. 3 DSC pattern of PU non-ionomers and ionomers scanned from 0°C to 240°C at a heating rate of 20 K/min

The DSC cooling scans (Fig. 4) show that the crystallization exothermic peaks of soft segment and hard segment appear for sample 60-0 without DMPA, suggesting the existence of phase separation structure. However, the introduction of DMPA on hard segment causes the disappearance of crystallization exothermic peaks of soft segment and hard segment as shown by results of PU non-ionomer series. Instead, for PU ionomer series, when the DMPA content is higher than 10 wt% such as samples 60-10I and 60-13I, the crystallization exothermic peak of soft segment could be observed, suggesting that the ionic groups with high concentration on hard segment could facilitate the phase separation which increases the crystallibility of the soft phase.

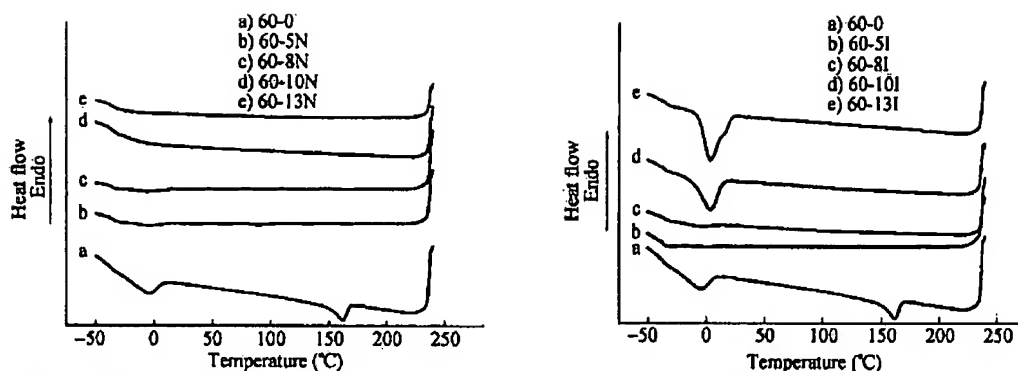


Fig. 4 DSC pattern of PU non-ionomers and ionomers scanned from 0°C to 240°C at a cooling rate of 20 K/min

#### Dynamic Mechanical Analysis

Figures 5 and 6 show the tensile storage modulus  $E'$  from dynamic mechanical analysis of PU non-ionomer and ionomer series. It found that there is a large difference in modulus below and above the transition temperature, which renders a sharp transition to the shape memory materials. The crystallization state of soft domain gives the high modulus at temperatures below  $T_m$ , whereas the entropy elasticity of molecular chain and physical crosslinks among hard segments cause the rubbery state modulus when the temperature increases beyond the transition temperature. In non-ionomer series, with the increase of DMPA content, the storage modulus  $E'$  at the temperature range above  $T_m$  is decreased abruptly which could be attributed to the disruption of ordered structure of hard domain with the introduction of the asymmetrical extender. Meanwhile, in the ionomer series studied, with the increase in DMPA content, the  $E'$  at the temperature higher than  $T_m$  is decreased firstly and subsequently increased when the DMPA content is higher than 5 wt%, suggesting that charged ionic group could enhance the cohesion among the hard segments in comparison with the corresponding PU non-ionomer especially in the PU ionomer samples with high ionic group content. The effect of increased cohesion among hard segments could be observed clearly from a comparison between PU non-ionomer and ionomer in Fig. 7. Therefore, the two-fold effect of charged ionic groups on the hard domain could be elucidated just like that reported by other researchers<sup>[16,17]</sup>. On the one hand, ionic groups on hard segment could cause the disruption of the ordered structure of hard domain; on the other hand, the cohesion between hard segments could be increased for the Coulombic force between the ionic groups on hard segments. One of the two factors could be dominant under different specific polyurethane molecular system.

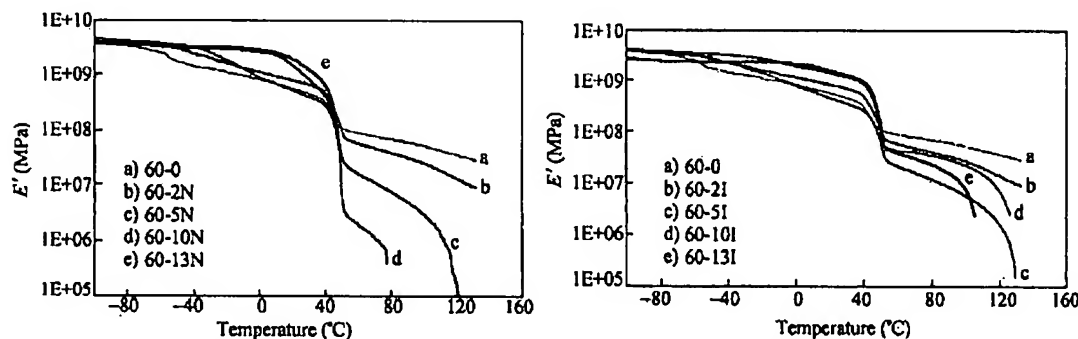
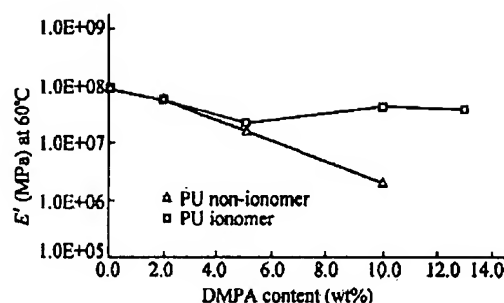
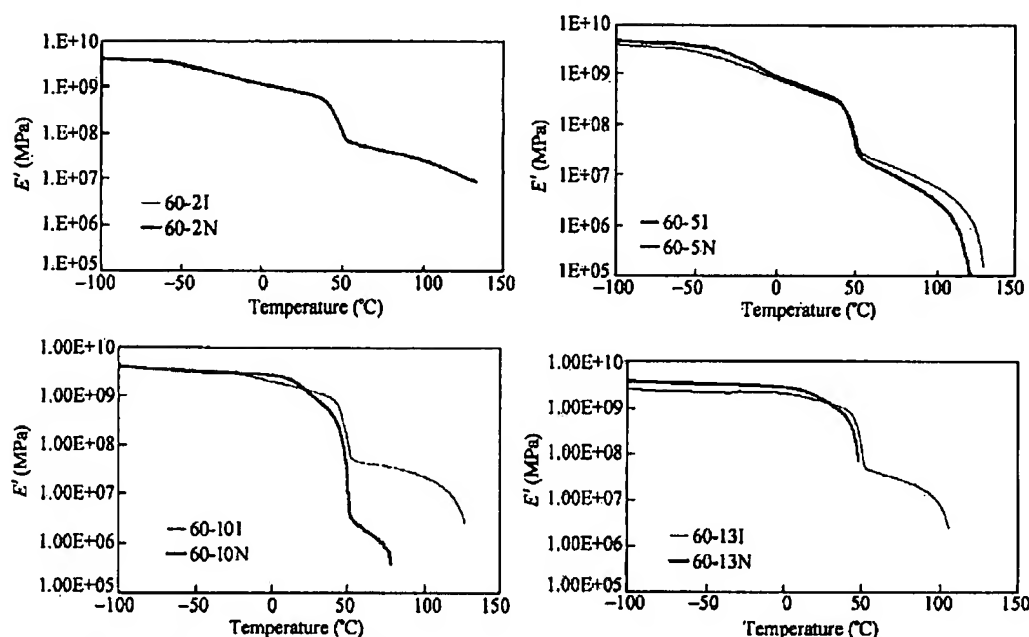


Fig. 5 Storage modulus  $E'$  of PU non-ionomer and the corresponding ionomer

Fig. 6 Comparison of  $E'$  at 60°C between PU non-ionomer and ionomer seriesFig. 7 Comparison of storage modulus  $E'$  of PU non-ionomer and the corresponding ionomerTable 3.  $T_g$  of soft segment from dynamic mechanical curves of films

Sample No.	60-0	60-2N	60-5N	60-10N	60-13N
$T_g$ (°C)	-75.0	-52.0	-35.5	10.0	18.0

Sample No.	60-0	60-2I	60-5I	60-10I	60-13I
$T_g$ (°C)	-75.0	-60.0	-58.0	-25.5	2.4

The glass transition of soft segment could be determined from the maxima of the loss modulus  $E''$  as shown in Fig. 8 and Table 3. Glass transition temperature of soft segment ( $T_{gs}$ ) of the two series exhibits the similar trend that the  $T_{gs}$  increases with the increase in DMPA content, suggesting the introduction of ionic group, whether neutralized or not, could disrupt the ordered hard domain and cause more hard segment to be dissolved in the soft segment phase whereas  $T_{gs}$  of PU ionomer is lower than the corresponding PU non-ionomer. The location of  $T_{gs}$  is sometimes used as indicators of phase purity in multi-block polyurethanes. If the copolymer is assumed to behave like a blend of homopolymers, the  $T_g$  of the phases in the blend could be compared to those of the neat components to determine the degree of hard/soft segment mixing<sup>[18,19]</sup>. Therefore, in terms of the lower  $T_{gs}$  of PU ionomer compared with that of corresponding PU non-ionomer, it could be tentatively

concluded that there are more hard-segment mixing in the soft segment phase in PU non-ionomer in comparison with that of the corresponding ionomer, which suggests that charged ionic groups on hard segment could improve the micro phase separation by enhancing the cohesion of hard segment.

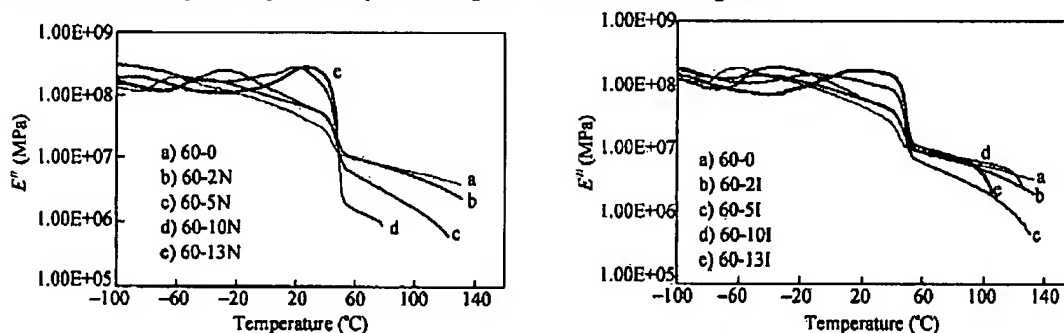


Fig. 8 Plots of loss modulus  $E''$  of PU non-ionomer and the corresponding ionomer

#### IR Analysis

To investigate the effect of charged ionic groups on hard segment on the micro phase separation, infrared spectra were used to analyze the carbonyl absorption for PU non-ionomer and ionomer. The hydrogen bonding is characterized by a frequency shift of bonded carbonyl groups to values lower than those corresponding to the free carbonyl groups. Xu *et al.*<sup>[20]</sup> reported the IR spectrum of PU synthesized with PCL, MDI and BDO, in which,  $1730\text{ cm}^{-1}$  and  $1701\text{ cm}^{-1}$  are assigned as the free and hydrogen bonded carbonyls of hard segments respectively. Meanwhile the corresponding vibration frequencies for carbonyls of soft segment are located at  $1735\text{ cm}^{-1}$  and  $1706\text{ cm}^{-1}$  respectively. Kim<sup>[14]</sup>, Ten-Chin Wen<sup>[21]</sup> *et al.* have previously reported that the band centered at  $1665\text{ cm}^{-1}$  is assigned to the stretching vibration of hydrogen-bonded carboxylic carbonyl group in PU, which comes from DMPA unit. Therefore, the extent of hydrogen bonding could be studied through the analysis of stretching vibration band of carbonyl group ( $1650\text{--}1740\text{ cm}^{-1}$ ) in IR spectrum.

From Fig. 9, it could be seen that the carbonyl stretching vibration is shifted to higher frequency with the increase of DMPA content whether in the non-ionomer or the ionomer series, indicating there might exist two possibilities: (i) more free carbonyl groups are produced; (ii) the reduction of ordered structure of hard domain. From the results of DMA, it was tentatively concluded that more phase mixing was produced with adding DMPA, which means the fraction of free carbonyl groups in the soft phase is reduced. Therefore, we presume that there is a more disordered structure or free carbonyl groups produced in the hard phase, which may surpass the effect of reduction of the fraction of free carbonyl groups in the soft phase and cause the shift of carbonyl stretching vibration to high frequency region. It might demonstrate, with the introduction of asymmetrical extender with neutralization or not, the effect of the disruption of ordered hard domain, caused by DMPA is predominant.

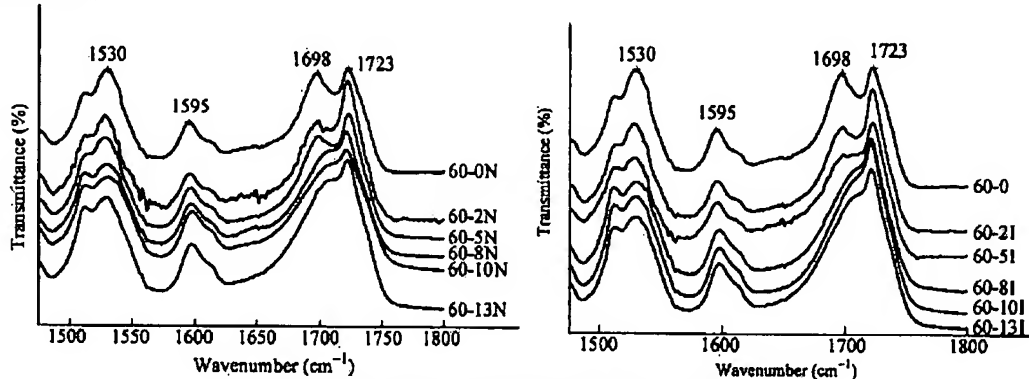


Fig. 9 IR spectra of PU non-ionomer series and ionomer series

Through the comparison between the carbonyl regions at IR spectra of PU non-ionomer and the corresponding ionomer, the effect of ionic groups on phase separation could be studied. As shown in Fig. 10, there is not significant difference between PU non-ionomer and the corresponding ionomer when DMPA content is low (2 wt%) or high (12.6 wt%). However, when DMPA content is 5 wt%–10 wt%, the charged ionic groups cause an obvious shift of carbonyl group stretching vibration to high frequency. It might be concluded that the fraction of free carbonyl groups is increased after neutralization which might be caused by enhanced phase separation, which agrees well with the resulting data about  $T_g$  of soft phase with DMA, in which, the  $T_g$  of samples with 5 wt% and 10 wt% DMPA content, is decreased significantly after neutralization with TEA. For samples, 60-13N and 60-13I, it is difficult to give a reasonable explanation about the similar IR spectra of the non-ionomer and ionomer. It might be the result of counteraction of two opposite factors induced by strong Coulombic force between ionic groups on the hard segment.

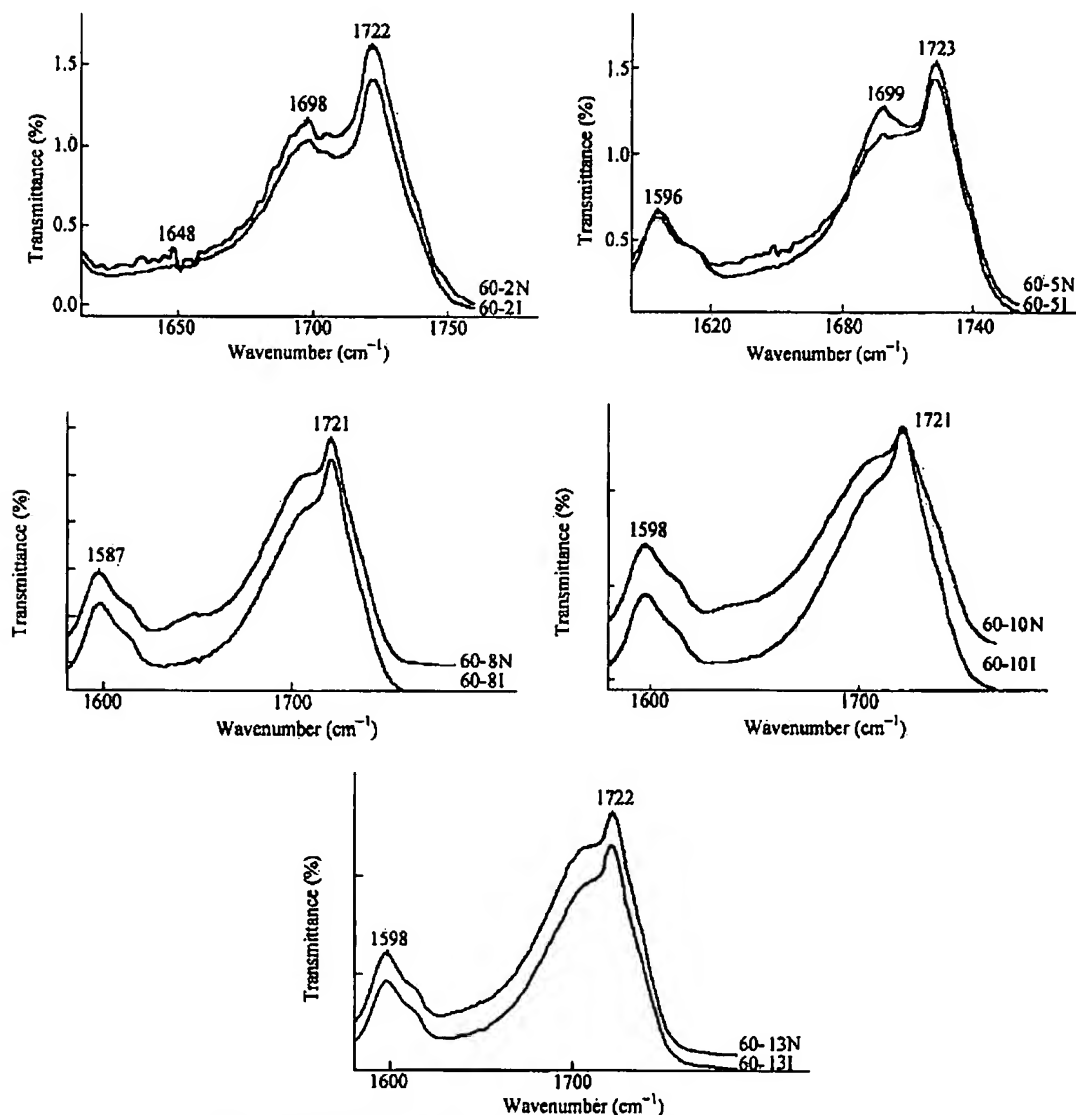


Fig. 10 Comparison of IR spectra between PU non-ionomers and ionomers

### Cyclic Thermo-Mechanical Investigation

#### Cyclic tensile test

The shape memory effect of segmented polyurethane could be studied with cyclic tensile test (Figs. 1 and 12), in which the cyclic hardening, caused by the orientations of PU segments during extension, can be observed. This cyclic hardening and even the shape of stress-strain curves are mostly confined to the first several cycles and no significant change is observed with further cycles<sup>[2]</sup>. Figure 11 shows the stress at 100% elongation at the second tensile cycle of PU non-ionomers and ionomers. From the analysis in the study with DMA and FTIR, it is found that the introduction of asymmetrical extender causes the disruption of ordered hydrogen bonded hard domains which are usually considered as the physical crosslinking structure in the two phase morphology and contributed to the thermal stimulated deformation recovery<sup>[1-4,12]</sup>. Therefore, the shape memory effect of the PU non-ionomer and the ionomer series is supposed to be affected by their ionic group content.

From Figs. 11 and 12, it could be observed that the stress at 100% elongation of PU non-ionomer series at high temperature (60°C) is decreased sharply with the increase in DMPA content; instead, that value of PU ionomer series is relative steady. This result is in agreement with the analysis above: the introduction of DMPA could disrupt the ordered hard domain, which offers the physical crosslink in the fixed phase. Meanwhile, charged ionic groups could enhance the cohesion between hard segments which has been characterized by DMA. With the increase of charged ionic groups in the ionomer series, especially for PU ionomer with DMPA content higher than 10 wt%, the total strain recovery ratio ( $R_{t, tot}$ ) decreases greatly from 83.41% (sample 60-2I: 2 wt% DMPA content at the first cycle test) to 61.59% (sample 60-13I: 13 wt% DMPA content at the first cycle test) and the recovery fixity ratio ( $R_f$ ) could be kept in a high level at around 93% that might stem from the strong crystallizability of ionomer series as shown in DSC cooling scan in Fig. 4. For all the specimen studied, the strain recovery ratio  $R_f(N)$ , reflecting the strain recovered in the following shape memory transition, could reach high level such as 97% or more after 3 or 4 testing cycle, which will be useful for some application area.

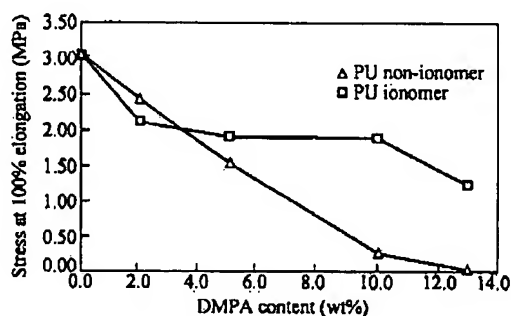
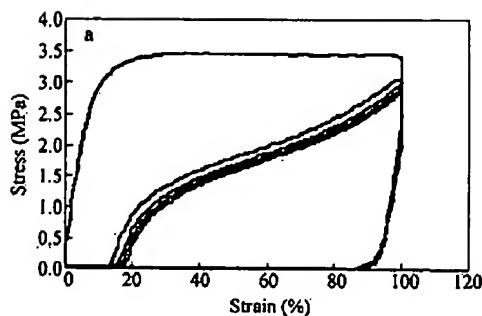
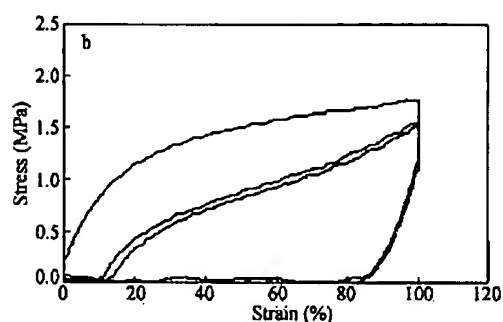


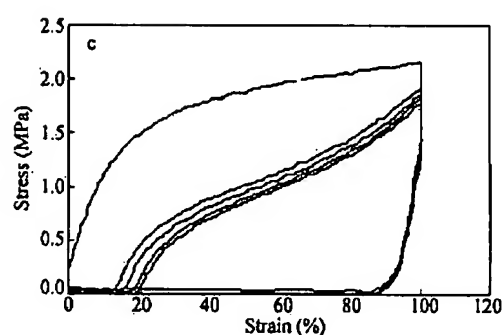
Fig. 11 Comparison of stress at 100% elongation of second tensile cycle between PU non-ionomers and ionomers



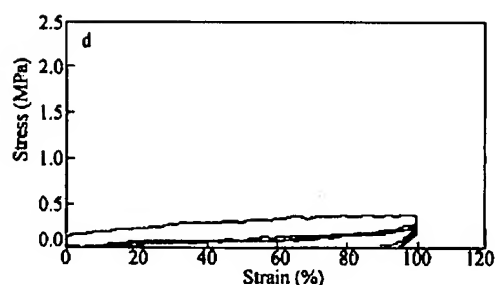
60-0	$\epsilon_p$ (%)	$1 - \epsilon_p$	Stress at 100% elongation (MPa)	$R_{t, tot}$ (N)	$R_f$ (N)
1	13.24	92.70	3.44	86.76	86.76
2	15.08	92.96	3.05	84.92	97.88
3	16.59	92.70	2.96	83.41	98.22
4	16.75	92.83	2.90	83.25	99.81
5		92.82	2.85		



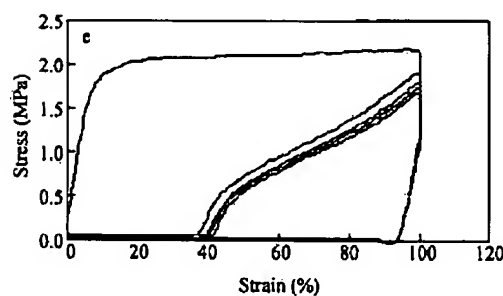
60-5N	$\epsilon_p$ (%)	$1 - \epsilon_a$	Stress at 100% elongation (MPa)	$R_{r,100}$ (N)	$R_r$ (N)
1	9.11	87.23	1.77	90.89	90.89
2	13.23	87.12	1.55	86.77	95.47
3			1.5		
4					
5					



60-5I	$\epsilon_p$ (%)	$1 - \epsilon_a$	Stress at 100% elongation (MPa)	$R_{r,100}$ (N)	$R_r$ (N)
1	13.25	92.25	2.14	86.75	86.75
2	16.58	92.24	1.9	83.42	96.16
3	18.25	92.25	1.85	81.75	98.00
4	19.95	92.49	1.82	80.05	97.92
5		92.27	1.78		



60-10N	$\epsilon_p$ (%)	$1 - \epsilon_a$	Stress at 100% elongation (MPa)	$R_{r,100}$ (N)	$R_r$ (N)
1		94.51	0.37		
2		93.90	0.27		
3		93.79	0.24		
4		93.88	0.23		
5					



60-10I	$\epsilon_p$ (%)	$1 - \epsilon_a$	Stress at 100% elongation (MPa)	$R_{r,100}$ (N)	$R_r$ (N)
1	36.74	93.92	2.14	63.26	63.26
2	39.90	93.83	1.89	60.10	95.00
3	40.07	93.83	1.8	59.93	99.72
4	41.75	93.76	1.74	58.25	97.20
5		93.80	1.69		

Fig. 12 Cyclic tensile test of PU non-ionomers and ionomers  
a) 60-0; b) 60-5N; c) 60-5I; d) 60-10N; e) 60-10I

### Strain recovery test

Deformation recovery properties of PU non-ionomer and the ionomer series could be investigated by strain recovery test as shown in Fig. 2. The specimens for this test were prepared as those used in cyclic tensile test. The film is stretched to 100% elongation at 60°C, then cooled to room temperature (20°C) and kept under strain constraint for a fixed length time of (900 s) so as to fix the deformation. When the stretched specimen was released from the strain constrain at room temperature, the relaxation without any constrain at room temperature was conducted for different lengths of time in order to investigate the relaxation time dependence of strain recovery properties. In this test, only one sample 60-0 was tested and the resulting data are shown in Fig. 13. It elucidates that the deformation could be recovered quickly when the temperature is raised to switching temperature and most deformation recovery is finished in a narrow temperature range. Besides, the switching temperature is shifted to high temperature with the increase in relaxation time and the strain recovery curves are almost superposed, when the relaxation time is sufficiently long such as 48 h or more; the recovery ratio of the samples with different relaxation time is nearly the same. Therefore, it could be concluded that, with regard to the relaxation time, the switching temperature is increased to a steady status, and the recovery ratio is not changed significantly.

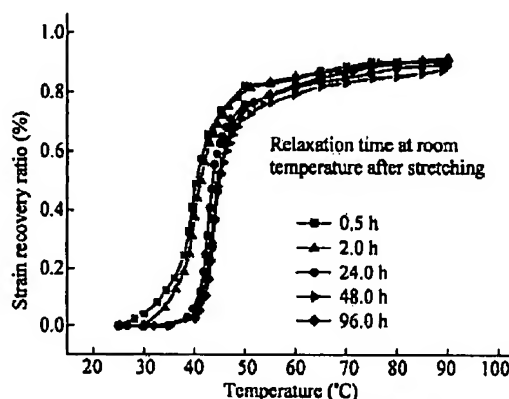


Fig. 13 Relaxation time dependence of strain recovery property of sample 60-0

Based on the result above, the stretched samples for this test were all kept for a long time beyond 100 h so as to reach the steady status after sufficient relaxation. Such measurement might be close to the application situation in some cases. Strain recovery curve is exhibited in Fig. 14 in which it could be found that the switching temperature is raised evidently with the increase of DMPA content for PU non-ionomer and the ionomer; the recovery ratio is decreased sharply for the non-ionomer but slightly lowered for the ionomer as shown in Fig. 15. The increase in switching temperature can be explained by the increase in  $T_m$  of the soft segment. For samples with high DMPA content, the hysteresis effect could be observed. After heating up to switching temperature, the samples, especially for 60-10I and 60-13I, still could undergo strain recovery to some extent until the highest temperature is reached. This hysteresis effect might be related to the disruption of ordered hard domains and the enhanced cohesion between hard segments.

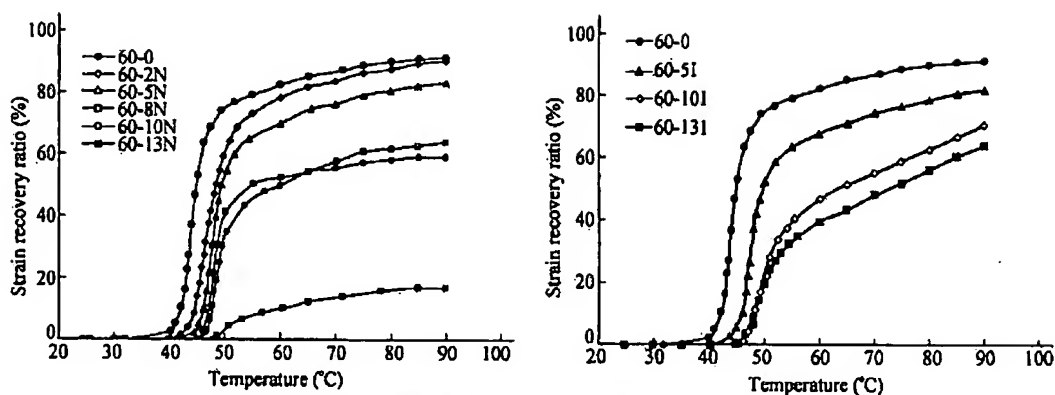


Fig. 14 Strain recovery test of PU non-ionomers and ionomers

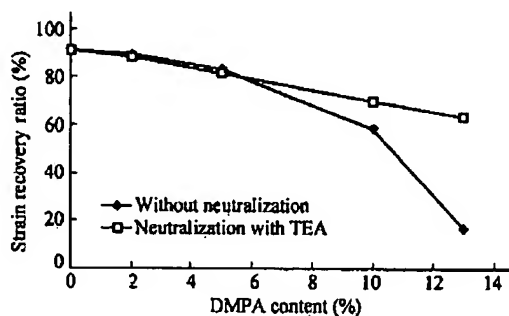


Fig. 15 Strain recovery ratio of PU non-ionomers and ionomers

## CONCLUSION

The PCL based polyurethane non-ionomer and the ionomer series were synthesized successfully. These two series of PU samples all exhibit the increased phase mixing with the DMPA content, and the charged ionic groups on hard segments could enhance the cohesion among hard segments and phase separation compared with the corresponding non-ionomers. The ionic groups on hard segments play two-fold effect: the disruption of ordered structure of hard domains and the enhance of cohesion among hard segments. When the ionic group content is moderate such as 5 wt%, the former effect is predominant; when the ionic group content is high enough, the cohesion among hard segments will be increased greatly and the latter effect becomes dominant. Therefore, the PU non-ionomer and ionomer series samples have different shape memory properties. With the introduction of asymmetrical extender, the stress at 100% elongation of the two series is decreased, especially lowered sharply for non-ionomer series because of the disruption effect for ordered structure of hard domains, which are usually regarded as physical crosslinking points in shape memory segmented PU. The Coulombic force in charged samples enhances the cohesion between hard segments, to some extent, supplementing the physical crosslinking points; the fixity ratio of ionomer series is not affected; the total recovery ratio of ionomer series is decreased greatly. After enough long relaxation time of stretched samples, the switching temperature is raised, whereas the recovery ratio is lowered with increased DMPA content for the two series PU samples. Thereby, in the molecular design of shape memory polyurethane ionomers, the complicated effect of ionic groups on shape memory effect and morphology of this kind of functional materials should be considered carefully.

## REFERENCES

- 1 Li, F.K., Zhang, X., Hou, J.A., Zhu, W. and Xu, M., *Acta Polymerica Sinica* (in Chinese), 1996, (4): 462
- 2 Kim, B.K. and Lee, S.Y., *Polymer*, 1996, 37: 5781
- 3 Kim, B.K., Lee, S.Y., Lee, J.S., Baek, S.H., Choi, Y.J., Lee, J.O. and Xu, M., *Polymer*, 1998, 39: 2803
- 4 Jeong, H.M., Ahn, B.K. and Kim, B.K., *European Polymer Journal*, 2001, 37: 2245
- 5 Tobushi, H., Hara, H., Yamada, E. and Hayashi, S., *Smart Materials and Structures*, 1996, 5: 483
- 6 Takahashi, T., Hayashi, N. and Hayashi, S., *Journal of Applied Polymer Science*, 1996, 60: 1061
- 7 Jeong, H.M., Ahn, B.K. and Kim, B.K., *Polymer International*, 2000, 49: 1714
- 8 Lendlein, A. and Kelch, S., *Angewandte Chemie International Edition*, 2002, 41: 2034
- 9 Tobushi, H., Hashimoto, T., Ito, N., Hayashi, S. and Yamada, E., *Journal of Intelligent Material Systems and Structures*, 1998, 9: 127
- 10 Hou, J., Ma, X., Luo, X., Ma, D., Zhang, X., Zhu, W. and Xu, M., "Thermally Simulated Shape Recovery Effect of Segmented Polyurethane," In: *Proceedings of The International Symposium on Polymer Alloys and Composites*, ed. by Choy, C.L. and Shin, F.G., Hong Kong Polytechnic University, Hong Kong, 1992, p.211
- 11 Li, F.K., Zhang, X., Hou, J.N., Xu, M., Luo, X.L., Ma, D.Z. and Kim, B.K., *Journal of Applied Polymer Science*, 1997, 64: 1511
- 12 Luo, X., Zhang, X., Wang, M., Ma, D., Xu, M. and Li, F., *Journal of Applied Polymer Science*, 1997, 64: 2433
- 13 Li, F., Chen, Y., Zhu, W., Zhang, X. and Xu, M., *Polymer*, 1998, 39: 6929
- 14 Yang, J.E., Kong, J.S., Park, S.W., Lee, D.J. and Kim, H.D., *Journal of Applied Polymer Science*, 2002, 86: 2375
- 15 Wei, X. and Yu, X. H., *Journal of Polymer Science: Part B: Polymer Physics*, 1997, 35: 225
- 16 Chen, S.A. and Chan, W.C., *Journal of Polymer Science: Part B: Polymer Physics*, 1990, 28: 1499
- 17 Kim, B.K. and Lee, J.C., *Polymer*, 1996, 37: 469
- 18 Garrett, J.T., Xu, R., Cho, J. and Runt, J., *Polymer*, 2003, 44: 2711
- 19 Sung, C.S.P., Hu, C.B. and Wu, C.S., *Macromolecules*, 1980, 13: 111
- 20 Xiao, F., Shen, D., Zhang, X., Hu, S. and Xu, M., *Polymer*, 1987, 28: 2335
- 21 Wen, T.C., Wu, M.S. and Yang, C.H., *Macromolecules*, 1999, 32: 2712